



ST. MARY'S
UNIVERSITY

Digital Commons at St. Mary's University


Honors Program Theses and Research Projects

Winter 11-21-2021

Synthesis and Characterization of Pyridine-Based Diimide Ligands and Metal Phosphonate Coordination Polymers

Juan Pinedo
jpinedo1@mail.stmarytx.edu

Follow this and additional works at: <https://commons.stmarytx.edu/honorsthesis>

 Part of the [Inorganic Chemistry Commons](#), [Materials Chemistry Commons](#), and the [Polymer Chemistry Commons](#)

Recommended Citation

Pinedo, Juan, "Synthesis and Characterization of Pyridine-Based Diimide Ligands and Metal Phosphonate Coordination Polymers" (2021). *Honors Program Theses and Research Projects*. 5.
<https://commons.stmarytx.edu/honorsthesis/5>

This Thesis is brought to you for free and open access by Digital Commons at St. Mary's University. It has been accepted for inclusion in Honors Program Theses and Research Projects by an authorized administrator of Digital Commons at St. Mary's University. For more information, please contact egoode@stmarytx.edu, sfowler@stmarytx.edu.

SYNTHESIS AND CHARACTERIZATION OF PYRIDINE-BASED DIIMIDE
LIGANDS AND METAL PHOSPHONATE COORDINATION POLYMERS

by

Juan L. Pinedo

HONORS THESIS

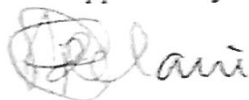
Presented in Partial Fulfillment of the Requirements for

Graduation from the Honors Program of

St. Mary's University

San Antonio, Texas

Approved by:



Dr. Pius O. Adelani

Thesis Supervisor



Dr. Camille Langston

Professor & Chair of Communication Studies
and Honors Director

November 21, 2021

© 2021

Juan Luis Pinedo

Abstract

By

Juan Luis Pinedo

Coordination polymers have become a topic of interest because these materials have a large variety of applications. A subclass of these materials are metal-organic frameworks (MOFs). MOFs have been researched due to their porosity and simple synthetic pathways. Structurally, a MOF is composed of one or more organic ligands serving as the backbone of the structure. These ligands are complexed with metal ions coordinating into the desired structure. It is this structure that gives way to a variable porosity useful for proton conductivity and material transport. By varying backbone size a framework can be customized for use in specific applications. This can either result to differences in distance between molecules or interpenetration of frameworks with each other. A bulkier backbone has been seen to decrease the catenation of frameworks and in turn increase the volume observed. On the other hand a less sterically hindered molecule results in more catenation thus increasing the surface area of the molecule. For these reasons we sought to synthesize a variety of ligands with different size backbones (Naphthalene, pyromellitic, biphenyl and perylene diimide) for the future synthesis of MOFs for proton conduction studies. Here we present the initial data from our research including the spectroscopic data for dipyrityl naphthalene diimide, dipyrityl pyromellitic diimide, dipyrityl biphenyl diimide, and dipyrityl perylene diimide.

This thesis is dedicated to Dr. Adelani and Dr. Chen. As well as all the other individuals both friends and family that have allowed me to continue my academic career and the many professors that have shaped my academic life.

Contents

Figures.....	6
Tables	8
Chapter 1: INTRODUCTION.....	10
Chapter 2: EXPERIMENTAL	22
2.1 Syntheses.....	22
Chapter 3: RESULTS AND DISCUSSION	26
3.1 Products.....	26
3.2 FT-IR Spectra.....	31
3.3 H-NMR and C13-NMR Spectrum	37
3.4 UV-Vis Spectra.....	41
3.5 $\{[(\text{CH}_3)_2\text{NH}_2]_2[\text{Zn}\{\text{O}_3\text{PC}_6\text{H}_2(\text{OH})_2\text{PO}_3\}]\}_n$ (5) Structure	45
Chapter 4: CONCLUSIONS.....	50
Chapter 5: REFERENCES.....	51

FIGURES

- Figure 1. Proposed pyridine-based diimide structures: N,N'-bis(4-pyridyl)-naphthalene diimide (1), N,N'-bis(4-pyridyl)-biphenyl diimide (2), N,N'-bis(4-pyridyl)-pyromellitic diimide (3), N,N'-bis(4-pyridyl)-perylene diimide (4)..16
- Figure 2. A set-up for refluxing apparatus in the presence of nitrogen.17
- Figure 3. The set-up for a refluxing apparatus in dimethyl formamide using a voltmeter.18
- Figure 4. A Mettler Toledo balance with four decimal places was used to mass all the reactants..19
- Figure 5. A Fisher Brand oven set to 110 degrees Celsius was used to dry all the glassware and samples after filtration..20
- Figure 6. A 1200°C Hybrid Furnace - Tube/Muffle 3-In-1 was used in the hydro/solvothermal synthesis of the coordination polymers in polytetrafluoroethylene-lined Parr 4749 autoclaves with a 23mL internal volume..21
- Figure 7. N,N'-bis(4-pyridyl)-naphthalene diimide compound.....27
- Figure 8. Pyromellitic diimide synthesized in DMF (left) and imidazole (right).28
- Figure 9. Biphenyl diimide synthesized in imidazole (top two and bottom right) and DMF (Bottom left).....29
- Figure 10. Infrared spectroscopy of the starting materials 4-aminopyridine (top-left) and 1,4,5,8-naphthalenetetracarboxylic dianhydride (top-right), and the N,N'-bis(4-pyridyl)-naphthalene diimide produced (bottom)31
- Figure 11. The Infrared spectra of 1,2,4,5-benzenetetracarboxylic dianhydride (top) and N,N'-bis(4-pyridyl)-pyromellitic diimide (3) compounds: refluxed in DMF (middle) vs. Imidazole (bottom) was taken and compared with each other to determine if they are the same compound32
- Figure 12. The FT-IR spectra of N,N'-bis(4-pyridyl)-biphenyl diimide (2) compound was taken for the crude product (refluxed in DMF) as well as the left over after vacuum filtration (top). The FTIR spectrum of pure 3,3',4,4'-biphenyl tetracarboxylic dianhydride (bottom spectrum)33
- Figure 13. FT-IR spectroscopy of the perylene-3,4,9,10-tetracarboxylic dianhydride (top) and the powder residue after refluxing 4-aminopyridine and perylene-3,4,9,10-tetracarboxylic dianhydride in DMF (middle) are almost identical. Synthesis in imidazole (bottom)

shows promising peaks hinting at N,N'-bis(4-pyridyl)-perylene diimide (4) compound.	34
Figure 14. H-NMR (top) and C13-NMR (bottom) study of N,N'-bis(4-pyridyl)-naphthalene diimide (1) confirmed the product.	37
Figure 15. H-NMR (top) spectrum of N,N'-bis(4-pyridyl)-pyromellitic diimide (3) (refluxed in DMF) with the excess peaks ascribed to minor impurities. The C13-NMR spectrum (bottom) also confirmed the formation of the target product	38
Figure 16. H-NMR and C13-NMR spectra of the N,N'-bis(4-pyridyl)-biphenyl diimide (2) (synthesized in DMF) (top). H-NMR and C13-NMR spectra of the impured product (synthesized in imidazole) (bottom)	39
Figure 17. The H-NMR and C13-NMR spectra for the synthesis of N,N'-bis(4-pyridyl)-perylene diimide (4) compound did not confirm the desired product. The peaks correspond to the acetone peaks	40
Figure 18. UV-Vis absorbance of N,N'-bis(4-pyridyl)-naphthalene diimide (1) shows peaks due to the aromatic pyridine side chain as well as the aromaticity of the naphthalene back bone	41
Figure 19. UV-Vis absorbance of N,N'-bis(4-pyridyl)-pyromellitic diimide (3) products (synthesized in DMF or Imidazole). These are expected to give the single large peak shown around 269 nm	42
Figure 20. UV-Vis absorbance of N,N'-bis(4-pyridyl)-biphenyl diimide (2) compound synthesized in imidazole or DMF– patterns from different batches are similar....	42
Figure 21. UV-Vis spectra of N,N'-bis(4-pyridyl)-perylene diimide (4) compounds indicate that the batches synthesized with imidazole are the same compound with the expected broad peaks at ~500 nm	43
Figure 22. The asymmetric unit of (I) in position 1 - x, 1 - y, 1 - z showing 50% displacement ellipsoids	45
Figure 23. View down [100] of the three-dimensional framework structure of (I) with the ZnO ₄ and PO ₃ C moieties shown as polyhedra. Color key: ZnO ₄ groups = cyan, PO ₃ C groups = magenta, oxygen = red, carbon = black, hydrogen = white. The (CH ₃) ₂ NH ₂ ⁺ cations are omitted for clarity.	46

TABLES

Table 1 Hydrogen Bond information for 1,4-dihydroxy-2,5-benzenediphosphate	48
Table 2 Crystallographic Data For $\{[(\text{CH}_3)_2\text{NH}_2]_2[\text{Zn}\{\text{O}_3\text{PC}_6\text{H}_2(\text{OH})_2\text{PO}_3\}]\}_n$ (5)	49

ACKNOWLEDGEMENTS

Over the course of my academic journey I have had the opportunity to work with a multitude of individuals that have shaped me as a scientist and human being. I would like to thank Dr. Pius Adelani for the guidance and support he provided while conducting my thesis research as well as afterward. Would also like to thank Dr. Richard Cardenas and Dr. Xinghai Chen for the advising they provided during my undergraduate study. I would like to thank the Welch Foundation for providing the funds necessary for me to conduct this research over the two years that I actively worked on this project. Finally, I would like to thank St. Mary's University for the continued support and guidance I have received over my four years in the honors program.

CHAPTER 1: INTRODUCTION

Coordination polymers have become a topic of interest because these materials have a large variety of applications. A subclass of these materials are metal-organic frameworks (MOFs). MOFs have been researched due to their porosity and simple synthetic pathways. Structurally, a MOF is composed of one or more organic ligands serving as the backbone of the structure. These ligands are complexed with metal ions coordinating into the desired structure. These coordination interactions are a result of ionic bonding between the metal cores and the ligands forming a structured molecule. For one of these coordination polymers to be considered a MOF it must have dimensionality greater than one dimension.

Ideally, a MOF is coordinated in 3D space to increase its effective surface area. The 3D structure of a MOF allows it to be used in applications such as gas adsorption and catalysis.¹ Individual properties of the compound can be altered by using different organic compound as ligands and exchanging the metal ions for ones of a different oxidation state. A more negative charged side chain on a ligand would allow for a stronger bond to the metal core coordinating the structure in a higher degree of order. This high degree of structural order is indicative of the crystallinity of MOFs. As opposed to other coordination polymers which are amorphous, MOFs are characterized by their crystal structure. As a result, they can be easily identified after synthesis via X-ray crystallography.

Other coordination polymers do not use metal ions as coordination molecules. In order to generate a structure with stronger bonding interactions between monomers covalent organic

frameworks (COFs) use organic molecules to coordinate the ligand structure.² Resulting frameworks of this type are characterized by retention of the bond geometry that the coordinating molecule had. The ligand used in the creation of coordination polymers also affects the structures' ability to hold guest molecules. A more rigid tetrahedral monomer results in a COF with a higher surface area than a trigonal monomer would produce. The tetrahedral structure limits the potential movement of the COF as well as allows for growth in four directions. This creates a higher degree of order as well as larger pores between ligand groups.

The ligands being coordinated to the central molecule also affect the surface area of the structure. While the research of COFs has been extensive in the areas of naphthalene diimides and pyromellitic diimides, these ligands are of a smaller size than the not as thoroughly researched perylene. A smaller ligand such as pyromellitic diimide results in a shorter chain per unit and a more compact structure. This results in a lower surface area than a COF constructed from perylene when the more rigid tetrahedral coordination is used. However as reported by Venkata Rao et. al. under the more flexible trigonal structure the smaller ligand provides a higher surface area.² When naphthalene was compared to these results it was seen that structures synthesized with it did not exhibit as high of a surface area as with the other two ligands. It can be inferred that as the middle ground in terms of size the naphthalene compound did not benefit from the flexibility of the pyromellitic diimide or the bulkiness seen with the perylene diimide.

The difference in surface areas can be attributed to the catenation of the structures. A structure is said to be catenated when its framework interpenetrates or interweaves together with other units of itself.³ This interlocking of structures results in a framework that has smaller pores and as a result less surface area to bind to guest molecules. In exchange for a decrease in

effective surface area, frameworks of this type have been seen to possess higher mechanical stability as the interwoven molecules support the surrounding framework. It is due to this property that coordination polymers can be designed for a multitude of functions. As demonstrated by Omar K. Farha et. al., adding a bulky group to the interior of the framework pore allows for the degree of catenation to be controlled.³ By introducing a bromine atom to the pores of frameworks made of dipyridine naphthalene diimide, as well as other ligands of different sizes, complexed with 4,4',4'',4'''-benzene-1,2,4,5-tetrayl-tetrabenzoic acid the structure of the resulting compound was altered. When using the non-brominated ligand, the catenation of the resulting framework demonstrated interweaving between structural units. Additionally, the framework constructed from naphthalene was interpenetrated in not only the x- and y-axis but the z-axis as well³. As naphthalene was the largest ligand complexed with the tetrabenzoic acid derivative it would indicate that the aromatic rings and bulky nature of the naphthalene lead to this type of interpenetration. Smaller size molecules seem to generate interwoven species in only the x- and y-directions. On the other hand, the complexes obtained from the brominated ligand resulted in no catenation and a larger size pore. This supports Omar's conclusion that catenation can be controlled by introducing steric hindrance to the structure. Further work can now be done with this hindrance in mind to construct coordination polymers that are better suited for their designated use.

In addition, the usage of two different organic ligands allows for the structure of the MOF to exceed a one-dimensional coordination. A main ligand is used to establish the structure of the polymer while a second smaller ligand is used as a strut establishing a higher order structure between two polymer chains.³ As described previously, this allows for a great amount of

customization in the structure of the compound. By using a ligand with a certain structure as a base the amount of connecting pillars that are complexed between them can be modified to allow for more porosity or stronger structural integrity. Ligands used as the pillars could also be modified to include charged functional groups for electrochemical and catalytic function. This pillaring also allows for otherwise one-dimensional structures to layer together to form a complex third-dimensional network. Adjusting the ligands used would result in a change in distance between base ligands culminating in a change in function. This further extends the adaptability of coordination polymers.

As a result of their tunable pores and aromatic properties, coordination polymers have been investigated for the removal of toxins from water sources. Toxic compounds are produced from a large variety of industrial and commercial sources. Waste products from manufacturing of plastics, and chemical products are washed away into bodies of water that are not only used by aquatic life as a habitat but also by humans as water for consumption and cleaning. Dyes from printing, textiles and paperwork also contaminate the water supply in a more noticeable way. Even small amounts of dyes affect the quality of water as a noticeable change in appearances results from these compounds. In addition many dyes used in industry are toxic or carcinogenic so an effective way to remove dyes from water is a necessity.⁴

Dyes are known to be a difficult material to remove as they are not easily degraded by sun light and are not susceptible to oxidation reactions in many cases. As Enamul Haque et. al. demonstrated, adsorption is a viable method for the removal of dyes from aqueous environment.⁴ They specifically indicate how methyl orange and methylene blue are examples of anionic and cationic dyes that pose a danger due to their toxicity. While traditional methods are effective at

removing dyes individually, Enamul and his coworkers sought to use MOF-235, $[\text{Fe}_3\text{O}(\text{terephthalate})_3(\text{DMF})_3][\text{FeCl}_4]$, to simultaneously remove both anionic and cationic dyes. The resulting efficiency was compared to activated carbon as a control. It was demonstrated that the MOF performed adequately even though a low level of porosity was expected due to little adsorption of nitrogen. This is significant because a high effective adsorption of dye would indicate that the framework is working in such a way that the dye is being bound outside of the pores. An adapted structure of the MOF could be used to increase effectiveness despite apparent porosity. MOF-235 demonstrated a higher adsorption of both anionic and cationic dyes than what was seen with the activated charcoal. This was attributed to the electrostatic interactions that are generated from the positive and negative charged structures of a MOF. This claim was further supported by the decrease in adsorption when the pH is altered.⁴ It is also likely that the aromatic rings in the dyes form Van der Waals interactions within the ligands making up the backbone of the MOF.

The adaptability provided by the structure of coordination polymers lends itself so well to the adsorption of molecules in an aqueous environment. Moreover, the customizability of the structure could be used to specifically target toxins in water while maintaining an easily recoverable form for disposal of the waste. This property could also be applied to gaseous waste such as that produced from the burning of compounds in industrial processes. The setting and bonding of components in electronics and mechanical equipment released harmful fumes that porous frameworks could serve to protect against.

Epoxy resins are an important part of the production of electrical equipment because of its strong mechanical performance and adhesive ability. However these resins have a low fire

resistance resulting in toxic gas emission.⁵ Lei Sang and his group members sought to use MOFs to suppress the toxic gases resulting from burning of resins. A coordination polymer known as a zeolitic imidazolate framework (ZIF), a class of MOFs with similar topology as zeolites, was used because of its thermal stability as opposed to other coordination polymers. The high nitrogen content coupled with the metal ions in the structure allows for stable bonds between molecules thus increasing the stability of the ZIF at high temperatures.⁵ This means that not only could a MOF serve to adsorb toxic gases in case of combustion but also provide a flame resistance that would make operation of equipment safer and more effective. Additionally, Lei Sang demonstrates that polyphosphazenes have flame retardant properties as they self-extinguish and limit the oxygen available in the case of a fire. The known issue with these compounds is they have a high cost and low output making a two factor compound an important step in reducing fire risk. Therefore, Sang sought to synthesize an iron 2-methylimidazole MOF wrapped in poly(cyclotriphosphazene-co-4,4'-sulfonyldiphenol (PZS) to study its flame-resistant properties. Sang et. al. demonstrated that when epoxides was complexed with the iron-based MOF, it show a higher stability above 386°C relative to the pure epoxy resins. The carbonization of the MOF framework serves to preserve the epoxide and limit the combustion of the resin reducing the emission of toxic compounds.

The imidazole rich structure of this MOF could also be studied and complexed with different metals to impart properties beneficial to different types of resins. The iron used in this MOF could undergo oxidation allowing for the possibility of +2 and +3 oxidation states. If the metal were to be replaced with a metal ion having a different oxidation state, the coordination of the ligands could be different. This would result in different structure and bonding scheme as

well as a differing complex with the polyphosphazene. A complex with different coordination pattern may result in better flame resistance under various conditions. As earlier described, coordination polymers such as MOFs have pores that could be modified to suppress smoke emissions more effectively. Introducing a charged group into the pores could possibly bind to the particles in smoke filtering any combustion that is not suppressed by the covering compound.

The overall aim of the projects presented in this thesis is to design varying ligands for use in the synthesis of coordination polymer. In addition, I also utilized 1,4-dihydroxy-2,5-benzenediphosphonate ligand to synthesis metal coordination polymer. In this study, I investigated four pyridine-based ligands (Figure 1) with naphthalene, biphenyl, and perylene diimide backbones. The rigid pyridine-diimide derivatives (consisting of rigid benzene, naphthalene, and perylene rings) could act as the pillar to link the metal cations into one to three-dimensional network structures. The planar aromatic rings could also maintain the rigid framework after the removal of solvent molecules to form a porous framework. In addition, the rigid aromatic rings could favor intra-ligand interactions and induce luminescent features.

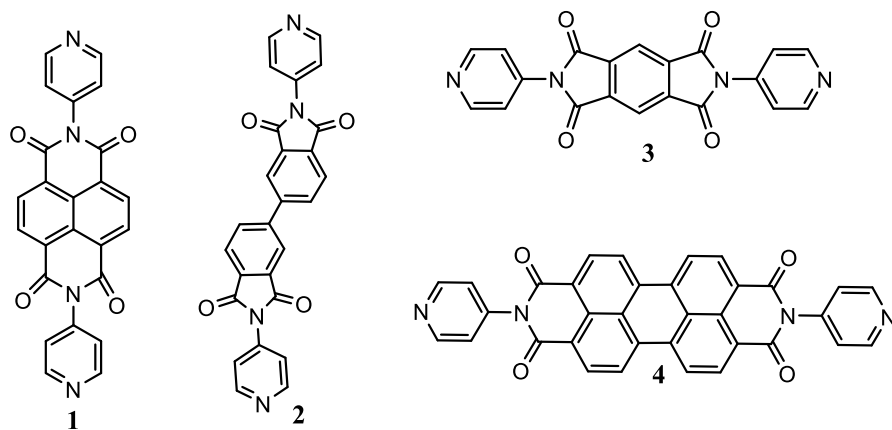


Figure 1: Proposed pyridine-based diimide structures: N,N'-bis(4-pyridyl)-naphthalene diimide (1), N,N'-bis(4-pyridyl)-biphenyl diimide (2), N,N'-bis(4-pyridyl)-pyromellitic diimide (3), N,N'-bis(4-pyridyl)-perylene diimide (4).

Diagram of Experimental Apparatus

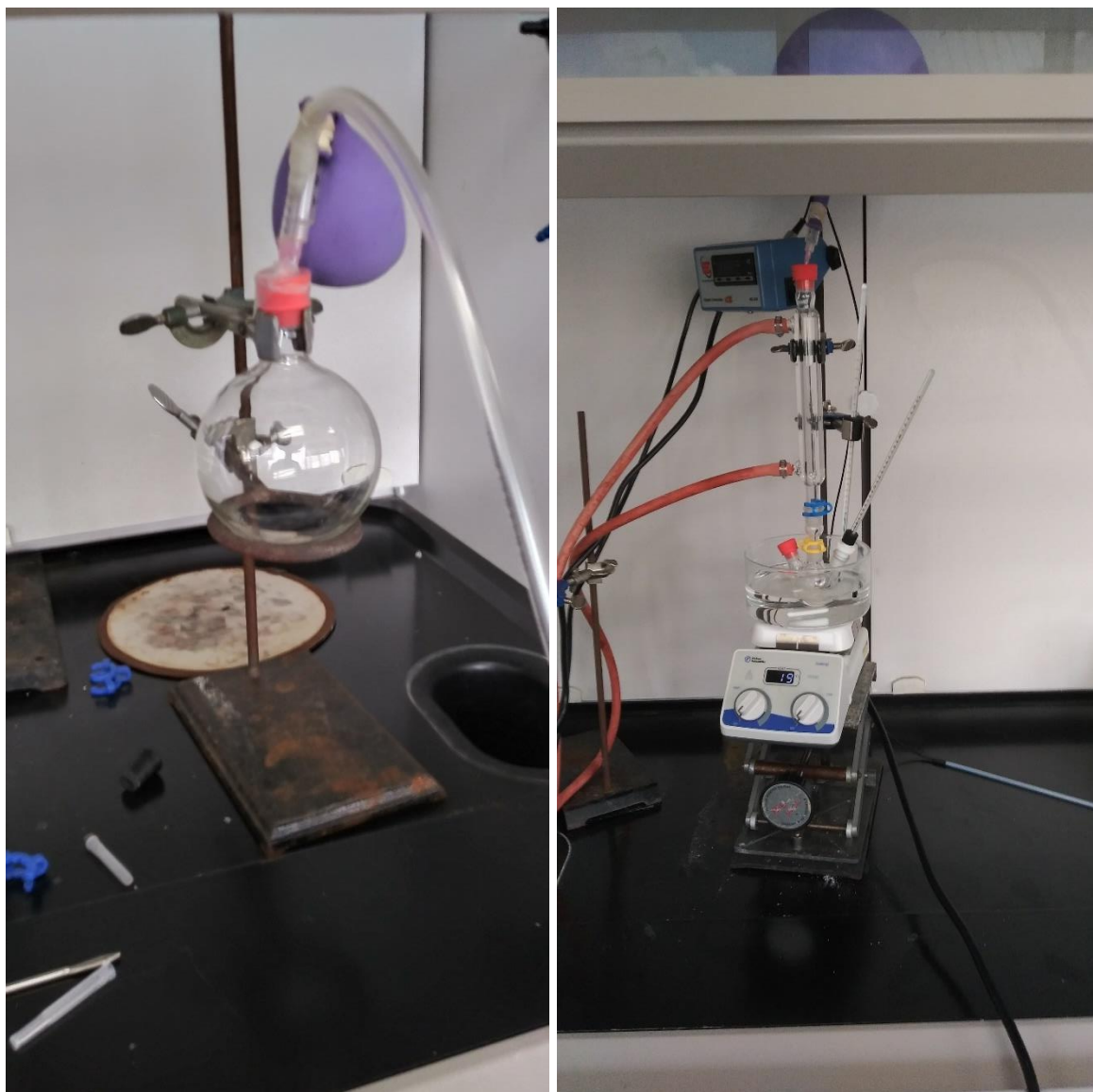


Figure 2: A set-up for refluxing apparatus in the presence of nitrogen.

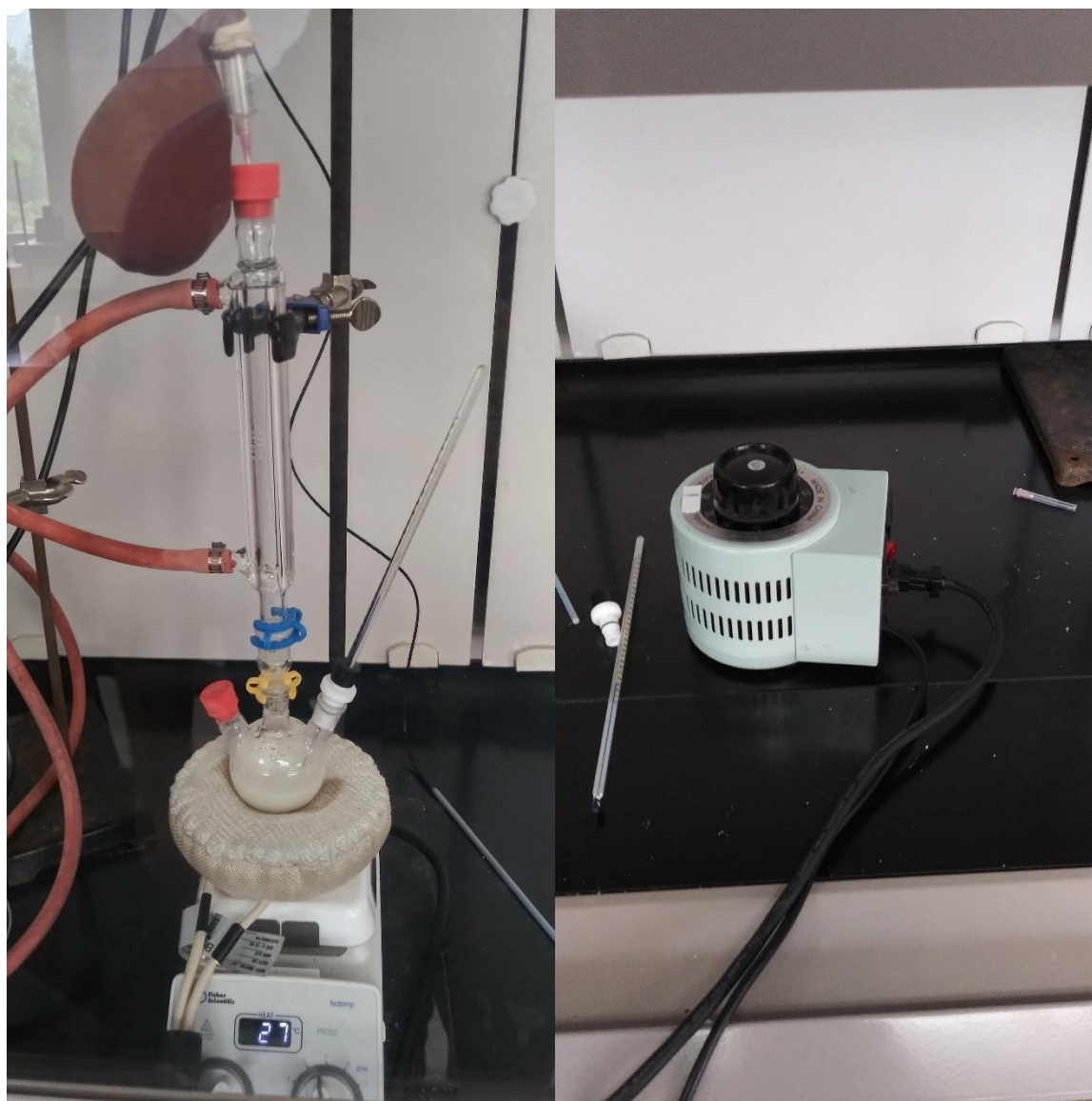


Figure 3: The set-up for a refluxing apparatus in dimethyl formamide using a voltmeter.



Figure 4: A Mettler Toledo balance with four decimal places was used to mass all the reactants.



Figure 5: A Fisher Brand oven set to 110 degrees Celsius was used to dry all the glassware and samples after filtration.

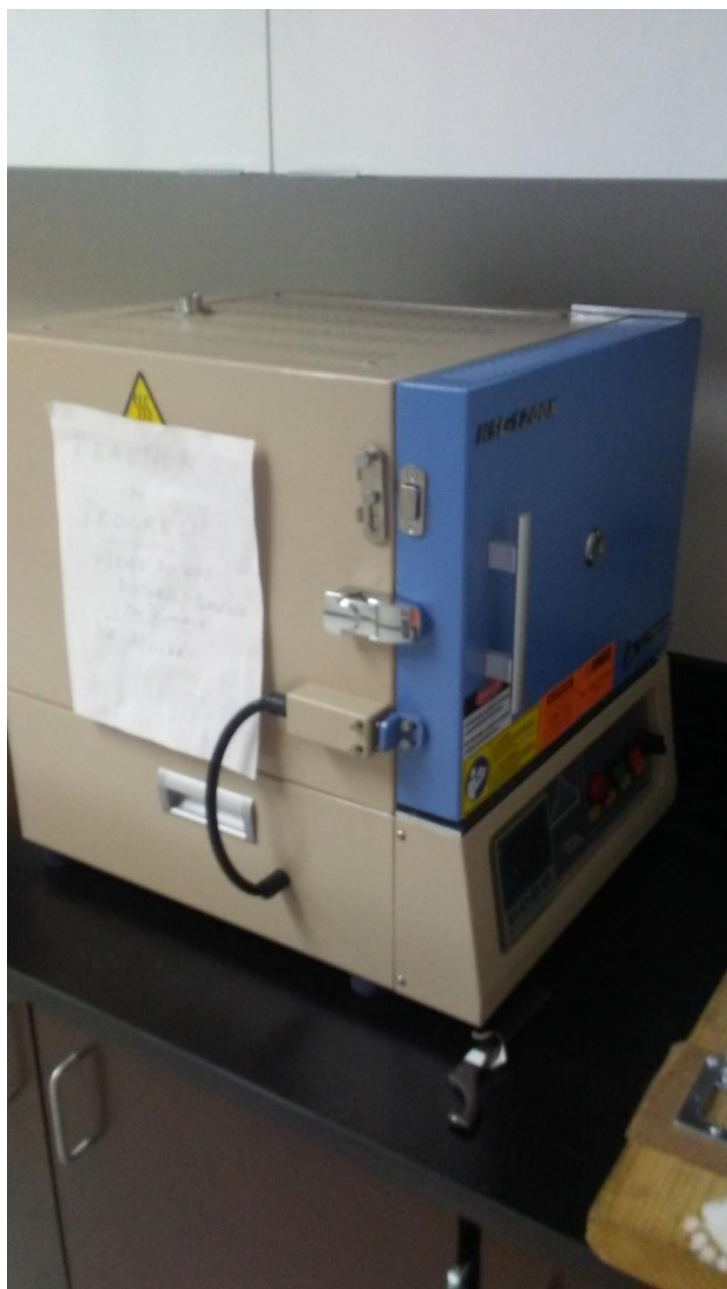


Figure 6: A 1200°C Hybrid Furnace - Tube/Muffle 3-In-1 was used in the hydro/solvothermal synthesis of the coordination polymers in polytetrafluoroethylene-lined Parr 4749 autoclaves with a 23mL internal volume.

CHAPTER 2: EXPERIMENTAL

2.1 Syntheses

Materials: All the reagents, 4-aminopyridine (99%, Sigma-Aldrich), benzene-1,2,4,5-tetracarboxylic dianhydride (97 %, Sigma-Aldrich), perylene-3,4,9,10-tetracarboxylic dianhydride (98 %, Sigma -Aldrich), 1,4,5,8-naphthalenetetracarboxylic dianhydride (97 %, Sigma-Aldrich), 3,3',4,4'-biphenyltetra-carboxylic dianhydride (97 %, Aldrich), 2,5-dihydroxy-1,4-benzenediphosphonic acid (98 %, Epsilon Chimie), imidazole (99.5%, Sigma-Aldrich), dimethylformamide (99.8% anhydrous, Sigma-Aldrich), and all other solvents were used without further purification.

Synthesis of N,N'-bis(4-pyridyl)-naphthalene diimide (1) using Imidazole. The compound was synthesized by reacting 1,4,5,8-naphthalenetetracarboxylic dianhydride (503.7 mg, 1.88 mmol) with 4-aminopyridine (543.4 mg, 5.77 mmol) in 2.0 g of molten imidazole. The mixture was heated under N₂ in an oil bath at 130°C for 30 min and allowed to cool to room temperature. The resulting solid was treated with a mixture of H₂O: EtOH: HNO₃ (10:10:1 ratio) and filtered. It was washed again with the same solution and then sequentially with cold H₂O, EtOH and Et₂O. The resulting product was a brown solid. This solid was then recrystallized in 150 mL DMF.¹ The spectroscopic characterization of the compound was then taken. The first

synthesis yielded about 219.0 mg (27% yield) and my second synthesis yielded 270.0 mg (34.2% yield).

Synthesis of N,N'-bis(4-pyridyl)-pyromellitic diimide (3) using DMF. 1,2,4,5-benzenetetracarboxylic dianhydride (1002.0 mg, 4.6 mmol) and 4-aminopyridine (1080.0 mg, 11.5 mmol) were added to a three-neck flask. Anhydrous dimethylformamide (DMF, 50 mL) was added under N₂, and the solution was refluxed overnight under N₂ at 130°C for 24 hours. After the reaction mixture was cooled in an ice bath, the white slurry was filtered, and the product was washed with CH₂Cl₂ and acetone. The product was further washed in DMF and allowed to dry in an oven at 110°C.⁶ The FT-IR was then taken and compared to the spectrum of the reactants. Proton and carbon-13 NMR were taken in DMSO, and UV-Vis absorbance was done in DMF. The product yielded 992.0 mg (58.3% yield) on my first synthesis and 1232.0 mg on the second synthesis.

Synthesis of N,N'-bis(4-pyridyl)-pyromellitic diimide (3) using imidazole. The synthesis was conducted using 1,2,4,5-benzenetetracarboxylic dianhydride (410.0 mg, 1.88 mmol) and 4-aminopyridine (543.4 mg, 5.77 mmol) in 2.0 g molten imidazole at 120°C for 30 mins in the same fashion as the N,N'-bis(4-pyridyl)-naphthalene diimide procedure. The first approach yielded ~57.0 mg (8.2 % yield). A 6.75 % yield was obtained (47.0 mg) on my second attempt and the yield improved on my third attempt to produce 22.8 % (159.0 mg).

Synthesis of N,N'-bis(4-pyridyl)-biphenyl diimide (2) using DMF. Using the same procedure as that for N,N'-bis(4-pyridyl)-pyromellitic diimide (3); 3,3',4,4'-biphenyl tetracarboxylic dianhydride (1354.0 mg, 4.6 mmol) and 4-aminopyridine (1078.0 g, 11.5 mmol)

were refluxed in 50 mL DMF at 120°C for 24 hours to produce an off white solid of about 716.5 mg (34.9 % yield). The resulting product was then characterized to confirm the structure.

Synthesis of N,N'-bis(4-pyridyl)-biphenyl diimide (2) using imidazole. The synthesis was conducted using 3,3',4,4'-biphenyl tetracarboxylic dianhydride (553.12 mg, 1.88 mmol) and 4-aminopyridine (543.4 mg, 5.77 mmol) in 2.0 g of molten imidazole in the same fashion as the N,N'-bis(4-pyridyl)-naphthalene diimide. A 126.8 mg yield (15.1%) was obtained from our first synthesis and the yield increased to 265.0 mg (31.6 %) was obtained from our second synthesis.

Synthesis of N,N'-bis(4-pyridyl)-perylene diimide (4) using imidazole. The synthesis was conducted using 3,4,9,10-perylenetetracarboxylic dianhydride (737.6 mg, 1.88 mmol) and 4-aminopyridine (543.4 mg, 5.77 mmol) in 2.0 g of molten imidazole in the same fashion as the N,N'-bis(4-pyridyl)-naphthalene diimide. A 1050.0 mg yield (104 percent) was obtained after my synthesis.

Synthesis of N,N'-bis(4-pyridyl)-perylene diimide (4) using DMF. The compound was synthesized in DMF by adopting the method reported by Pagano et al.⁷ 3,4,9,10-perylene-tetracarboxylic dianhydride (1804.6 mg, 4.6 mmol) and 4-aminopyridine (1082.4 mg, 11.5 mmol) were added to a three-necked flask and refluxed at 130°C for 72 hours in 50 ml of DMF under nitrogen gas. The mixture was then allowed to cool to 80°C. Thereafter, dichloromethane was added to the mixture and cooled down to room temperature. The solution was divided into 10 ml screw top centrifuge tubes and centrifuged at 4000 rpm for 45 minutes. The supernatant was decanted and disposed of. The remaining red solid was washed and filtered with diethyl ether. It was left in an oven at 110°C over night to dry. After analysis it was discovered that we did not produce the targeted product.

Synthesis of $\{[(\text{CH}_3)_2\text{NH}_2]_2[\text{Zn}\{\text{O}_3\text{PC}_6\text{H}_2(\text{OH})_2\text{PO}_3\}]\}_n$ (5). The compound was produced by adding $\text{Zn}(\text{NO}_3)_2 \cdot 6\text{H}_2\text{O}$ (29.7 mg, 0.1 mmol) and 2,5-dihydroxy-1,4-benzenediphosphonic acid (27.0 mg, 0.1 mmol) into a 125 ml PTFE-lined Parr reaction vessel along with DMF/ H_2O / ethanol (2.0/0.5/0.5 molar ratio, respectively). The vessel was heated in a programmable furnace (Figure 6) at 353 K for 3 days, and then the autoclave was cooled to 296 K at an average rate of 274 K per hr. The mother liquor was decanted from the products and then placed in a petri dish. The solid products were washed with distilled water, dispersed with ethanol, and allowed to dry in air. Colorless tablets of the title compound were isolated and studied for single-crystal X-ray diffraction.

NMR Spectroscopy: NMR was conducted on a Bruker 500 MHz Avance III HD instrument using deuterated DMSO as a solvent.

UV-Vis Absorbance: UV-Vis absorbance was collected in DMF for compounds 1, 2, and 3, while compound 4 was dissolved in DMSO.

CHAPTER 3: RESULTS AND DISCUSSION

3.1 Products

The synthesis of our target diimides was successful with minor problems along the way. It was believed that the synthetic technique we adopted with imidazole as a solvent was not adequate and caused our temperature control not to function appropriately. The volume of the solvent in the flask was not enough to cover our probe while the reaction was running. As a result, the internal temperature of the reaction was not well known. At times the reaction reached temperatures above 170°C thus leading to the decomposition of the product. This problem was not encountered when DMF was used as a solvent suggesting that the larger volume of solvent was a factor in controlling the internal reaction temperature of our reaction. N,N'-bis(4-pyridyl)-naphthalene diimide (**1**) synthesis was observed to proceed according to established reaction mechanisms. The resulting product was a light brown solid (see Figure 7) that was then analyzed via spectroscopy to determine the purity and success of the synthesis. I was also able to successfully synthesize N,N'-bis(4-pyridyl)-pyromellitic diimide (**3**). The resulting product was a white powder which was analyzed in the same way as described in compound **1** (see Figure 8). N,N'-bis(4-pyridyl)-biphenyl diimide (**2**) was synthesized as an off-white crystalline powder as shown in Figure 9. To obtain the spectroscopy of the sample it was ground into a fine powder before analysis. Based on the differing powder colors observed, we believe that the two methods of synthesis did result in similar product with differing amounts of impurities. It was also determined that using imidazole as a solvent for synthesis was not efficient as the yield was low

compared to the synthesis in DMF. An issue we faced with this synthesis was partial crystallization of the product during work-up. As a result, the product was separated into multiple parts and the spectroscopy of each part was taken. Products with similar spectroscopy were combined together into one storage bottle. Synthesis of N,N'-bis(4-pyridyl)-perylene diimide (4) resulted in a dark red compound when synthesized using imidazole and a bright red compound when synthesized with DMF.

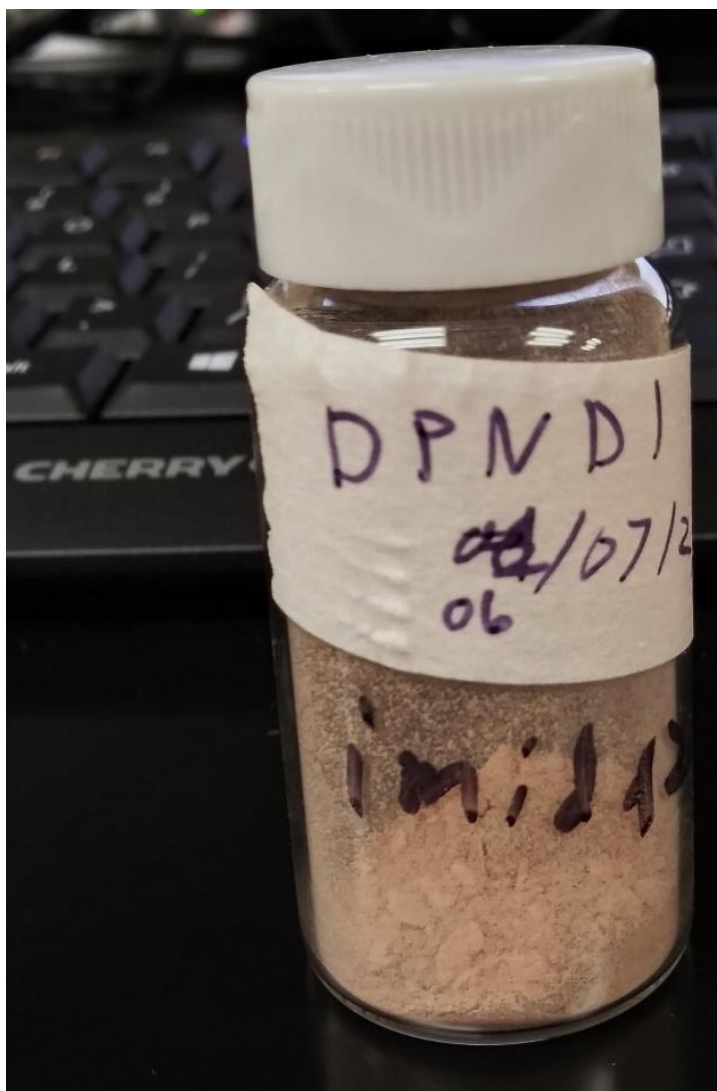


Figure 7. N,N'-bis(4-pyridyl)-naphthalene diimide compound.

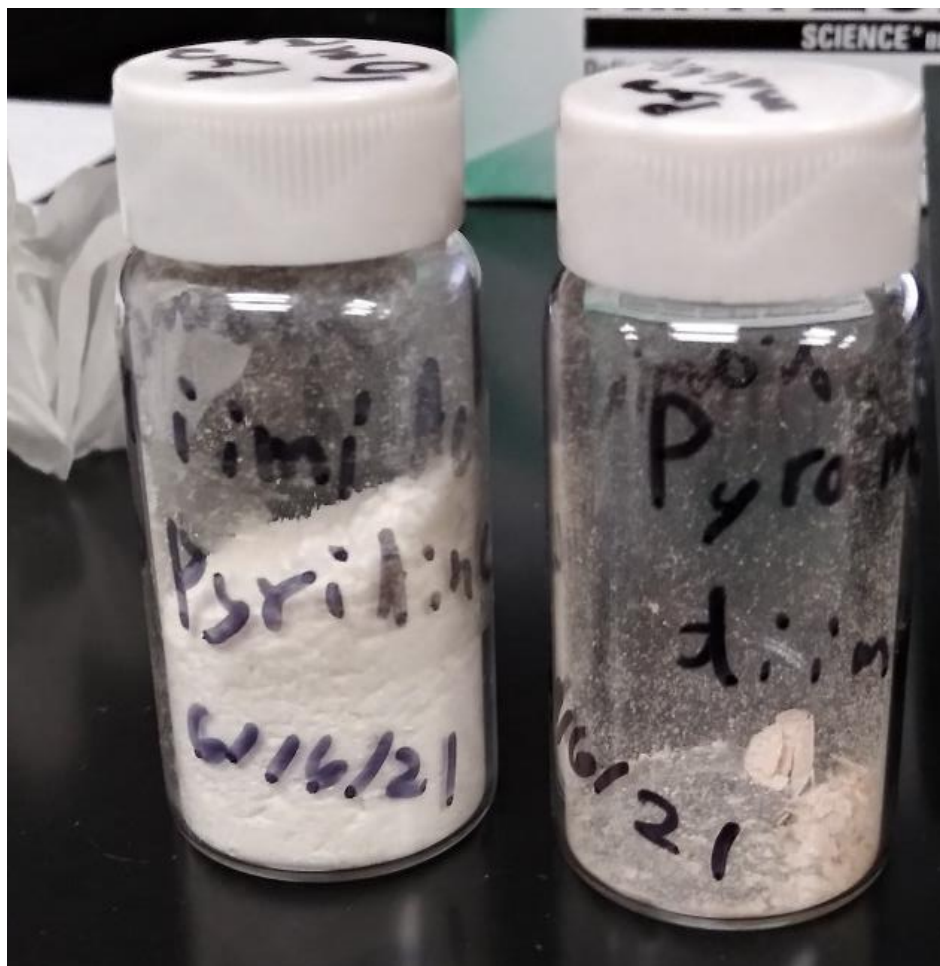


Figure 8: Pyromelic diimide synthesized in DMF (left) and imidazole (right).

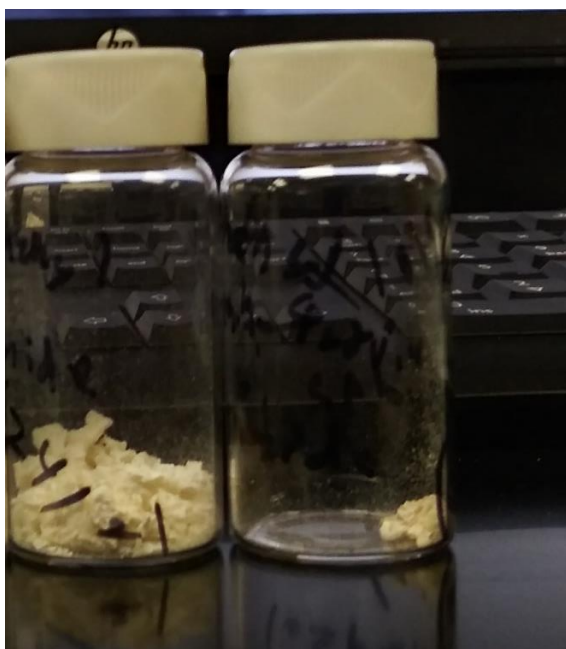


Figure 9: Biphenyl diimide synthesized in imidazole (top two and bottom right) and DMF (Bottom left)

The FT-IR spectra of the starting materials, 4-aminopyridine and 1,4,5,8-naphthalenetetra-carboxylic dianhydride were compared with the spectrum of the product, N,N'-bis(4-pyridyl)-naphthalene diimide (**1**), as shown in Figure 10. Based on the IR spectroscopy, it could be determined that the reactants bound correctly to form the product by the disappearance of the peak around 3500 cm^{-1} . This peak is attributed to the bond between the nitrogen and hydrogen atoms in the pyridine which is no longer present in the diimide structure. The twin peaks at 1712 cm^{-1} and 1671 cm^{-1} are indicative of the aromatic ring of the pyridine incorporated into the structure of diimide.

The FT-IR spectroscopy of N,N'-bis(4-pyridyl)-pyromellitic diimide (**3**) (see Figure 11) illustrated that the different synthetic methods resulted in differing products. For instance, when the synthesis was done with DMF, the products appear to be the same compound while the product synthesized with imidazole do not have similar peaks. It can be inferred from the peaks observed when DMF was used for the synthesis that the pyridine starting material was incorporated into the pyromellitic backbone. However, there are impurities and excess pyridine that need to be removed. Overall, the peaks around 1600 cm^{-1} for all products are indicative of the diimide product.

Both the FT-IR spectroscopy of the crude and the purified products of N,N'-bis(4-pyridyl)-biphenyl diimide (**2**) (see Figure 12) from DMF were the same compound. The disappearance of the prominent peak around 3500 cm^{-1} is indicative of the coupled pyridine with biphenyl dianhydride. The peaks around 2841.98 cm^{-1} are indicative of the diimide bonds to the biphenyl ring.

It was determined from the FT-IR spectroscopy (Figure 13) that the reaction in DMF was not successful. Spectrum analysis of imidazole-synthesized *N,N'*-bis(4-pyridyl)-perylene diimide (**4**) demonstrated promising peaks at 1768.71 cm^{-1} and 1665.34 cm^{-1} indicative of the pyridine being incorporated into the perylene backbone thus forming an imide.⁷ The absence of the peak at 3500 cm^{-1} that was seen in 4-aminopyridine spectrum also supports this conclusion.

3.2 FT-IR Spectra

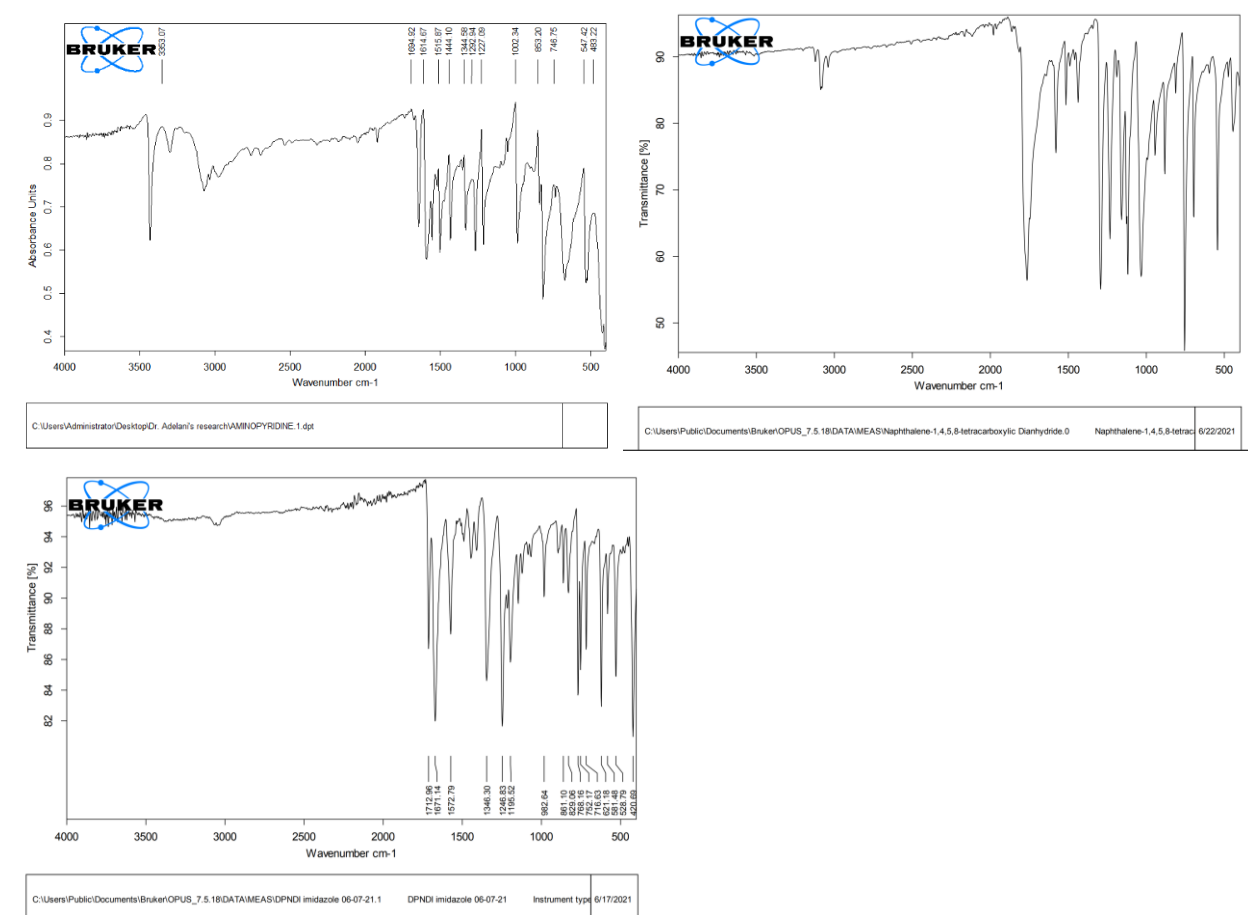


Figure 10: Infrared spectroscopy of the starting materials 4-aminopyridine (top-left) and 1,4,5,8-naphthalenetetracarboxylic dianhydride (top-right), and the *N,N'*-bis(4-pyridyl)-naphthalene diimide produced (bottom).

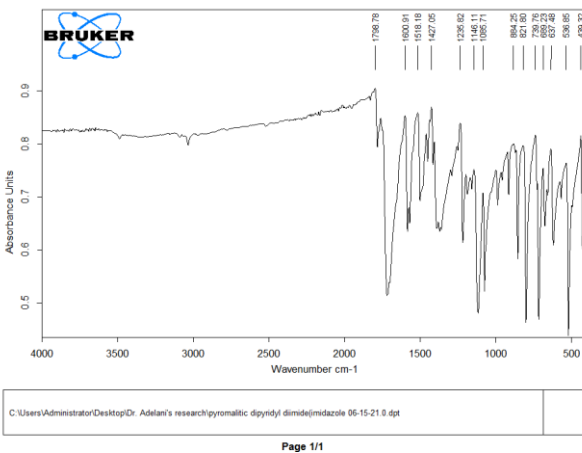
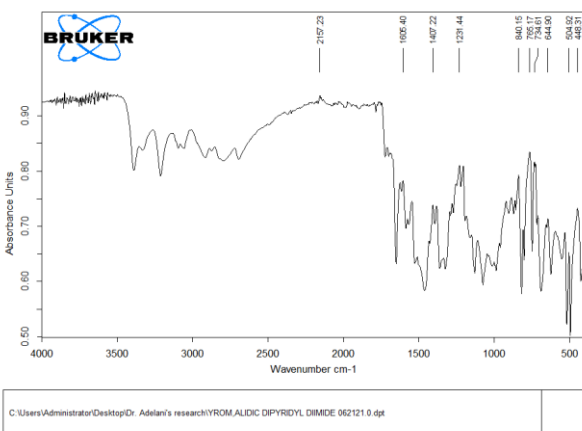
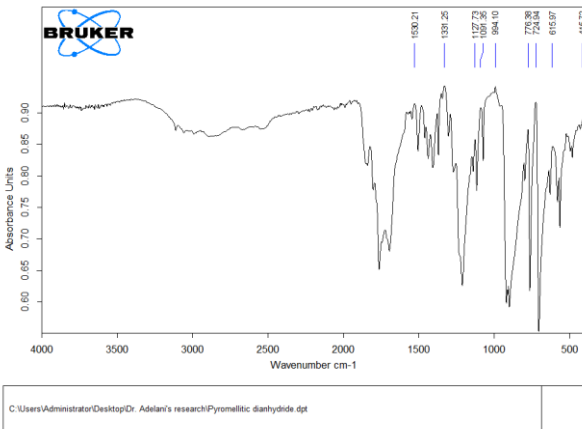
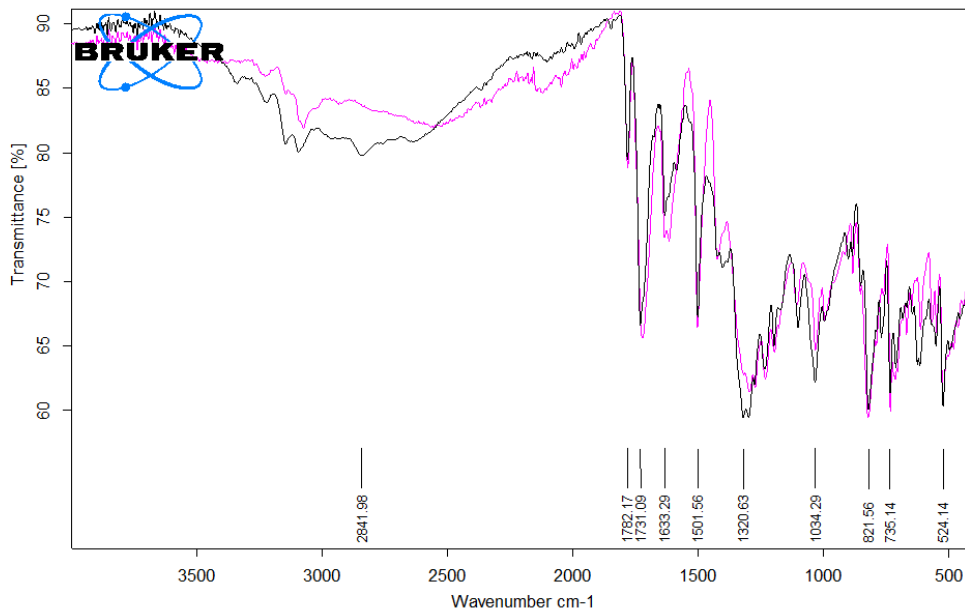
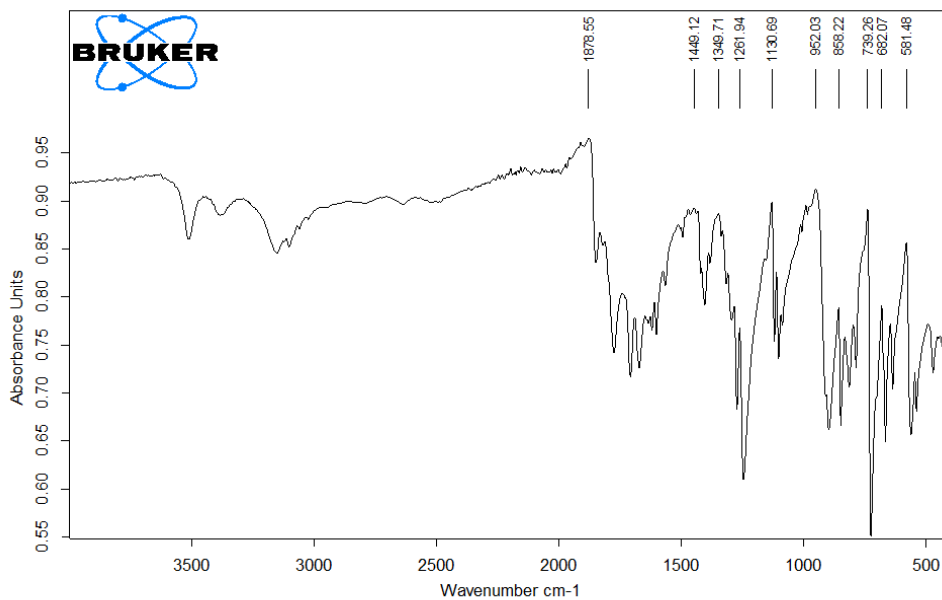


Figure 11: The Infrared spectra of 1,2,4,5-benzenetetracarboxylic dianhydride (top) and N,N'-bis(4-pyridyl)-pyromellitic diimide (3) compounds: refluxed in DMF (middle) vs. Imidazole (bottom) was taken and compared with each other to determine if they are the same compound.



C:\Users\Public\Documents\Bruker\OPUS_7.5.18\DATA\MEAS\BIPHENYL PYRIDINE DIIMIDE (RESIDUE) 07-2-21.0	BIPHENYL PYRIDINE	7/7/2021
C:\Users\Administrator\Desktop\Dr. Adelani's research\BIPHENYL PYRIDINE DIIMIDE 07 02 21 CRUDE.0.dpt		

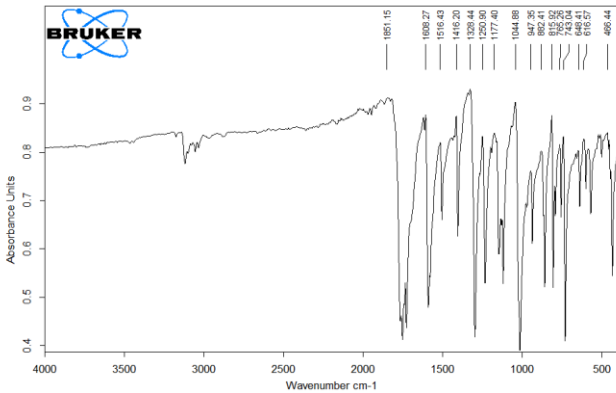
Page 1/1



C:\Users\Administrator\Desktop\Dr. Adelani's research\3,3,4,4-Biphenyltetracarboxylic dianhydride.dpt	
---	--

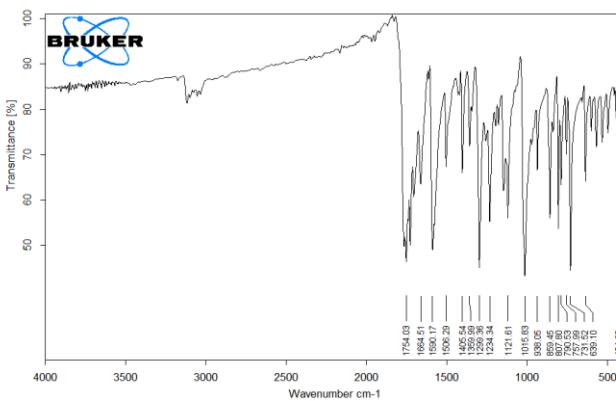
Page 1/1

Figure 12: The FT-IR spectra of N,N'-bis(4-pyridyl)-biphenyl diimide (2) compound was taken for the crude product (refluxed in DMF) as well as the left over after vacuum filtration (top). The FT-IR spectrum of pure 3,3',4,4'-biphenyl tetracarboxylic dianhydride (bottom spectrum).



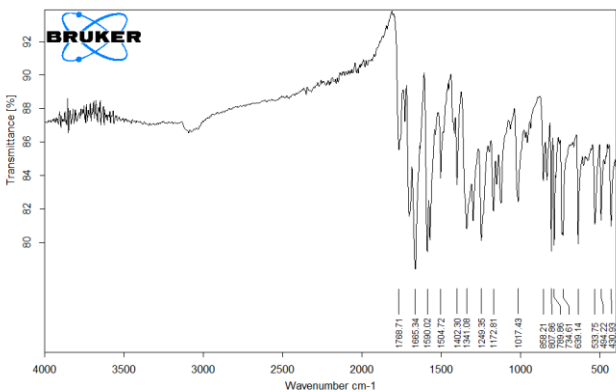
C:\Users\Administrator\Desktop\Dr. Adelan's research\Perylene-3,4,9,10-tetracarboxylic dianhydride.dpt

Page 1/1



C:\Users\Public\Documents\Bruker\OPUS_7.5.18\DATA\MEAS\dipyridyl-erylene dimide 07-13-21.0 dipyridyl-erylene dimide 07-13-21 7/19/2021

Page 1/1



C:\Users\Public\Documents\Bruker\OPUS_7.5.18\DATA\MEAS\dipyridyl-erylene dimide 07-19-21.0 dipyridyl-erylene dimide 07-19-21 7/21/2021

Page 1/1

Figure 13: FT-IR spectroscopy of the perylene-3,4,9,10-tetracarboxylic dianhydride (top) and the powder residue after refluxing 4-aminopyridine and perylene-3,4,9,10-tetracarboxylic dianhydride in DMF (middle) are almost identical. Synthesis in imidazole (bottom) shows promising peaks hinting at N,N'-bis(4-pyridyl)-perylene diimide (4) compound.

H-NMR spectroscopy was also conducted to characterize our compound. Singlet peaks at 7.58, 8.76, and 8.81 ppm (see Figure 14) indicate the structure of N,N'-bis(4-pyridyl)-naphthalene diimide (**1**) as previously reported by Stephanie Jenson.⁸ These peaks are due to the symmetrical structure of compound **1** leading to the integration of four hydrogens for the peak at 7.58 ppm, the hydrogens closest to the imide on the pyridine ring. The remaining peaks are attributed to the hydrogens on the naphthalene and the furthest hydrogens on the pyridine, respectively. C13-NMR however did not result in the expected 7 peaks of the symmetrical compound and instead only demonstrated one peak which is attributed to the solvent.

H-NMR study of N,N'-bis(4-pyridyl)-pyromellitic diimide (**3**) synthesized in DMF provided enough evidence to confirm the synthesized compound **3**. While there are some impurities in the sample, the peaks at 7.96, 8.11, and 8.85 ppm are indicative of compound **3** (see Figure 15).¹⁰ The peak at 7.96 ppm indicates the hydrogen atoms on the pyridine closest to the amide group on both side chains. The other peak at 8.11 ppm is attributed to the four furthest hydrogens on the pyridine ring while the peak at 8.85 ppm is consistent with the hydrogens on the benzene ring. C13-NMR also supports my claim since the six peaks shown correspond to the six peaks expected for compound **3**. The solvent peak were huge and thus reducing the visibility of the product peaks, but they can still be attributed to the symmetric structure of **3**.

Both proton and carbon-13 NMR spectra of N,N'-bis(4-pyridyl)-biphenyl diimide (**2**) shown in Figure 16 for imidazole-based synthesis of **2** confirm that the compound is not pure. There is a considerable amount of noise and excess peaks from solvent and impurities. The splitting seen in the H-NMR spectrum of DMF-synthesized product seems to be indicative of the hydrogen on the pyridine atoms as the doublet peaks are expected from protons close to each

other. The peaks at 6.5 ppm and 8.0 ppm are interpreted to be the hydrogens on the pyridine according to their proximity to the carbonyl group, respectively. The C13-NMR of this product is inconclusive as all that is observable is the solvent peak for the DMSO.

The NMR analysis of N,N'-bis(4-pyridyl)-perylene diimide as shown in Figure 17 was also inconclusive as neither the H-NMR nor C13-NMR spectrum displayed any peaks aside from the solvent peak and peaks attributed to impurities. I suspect some contamination resulting in acetone being introduced into our sample.

3.3 H-NMR and C13-NMR Spectrum

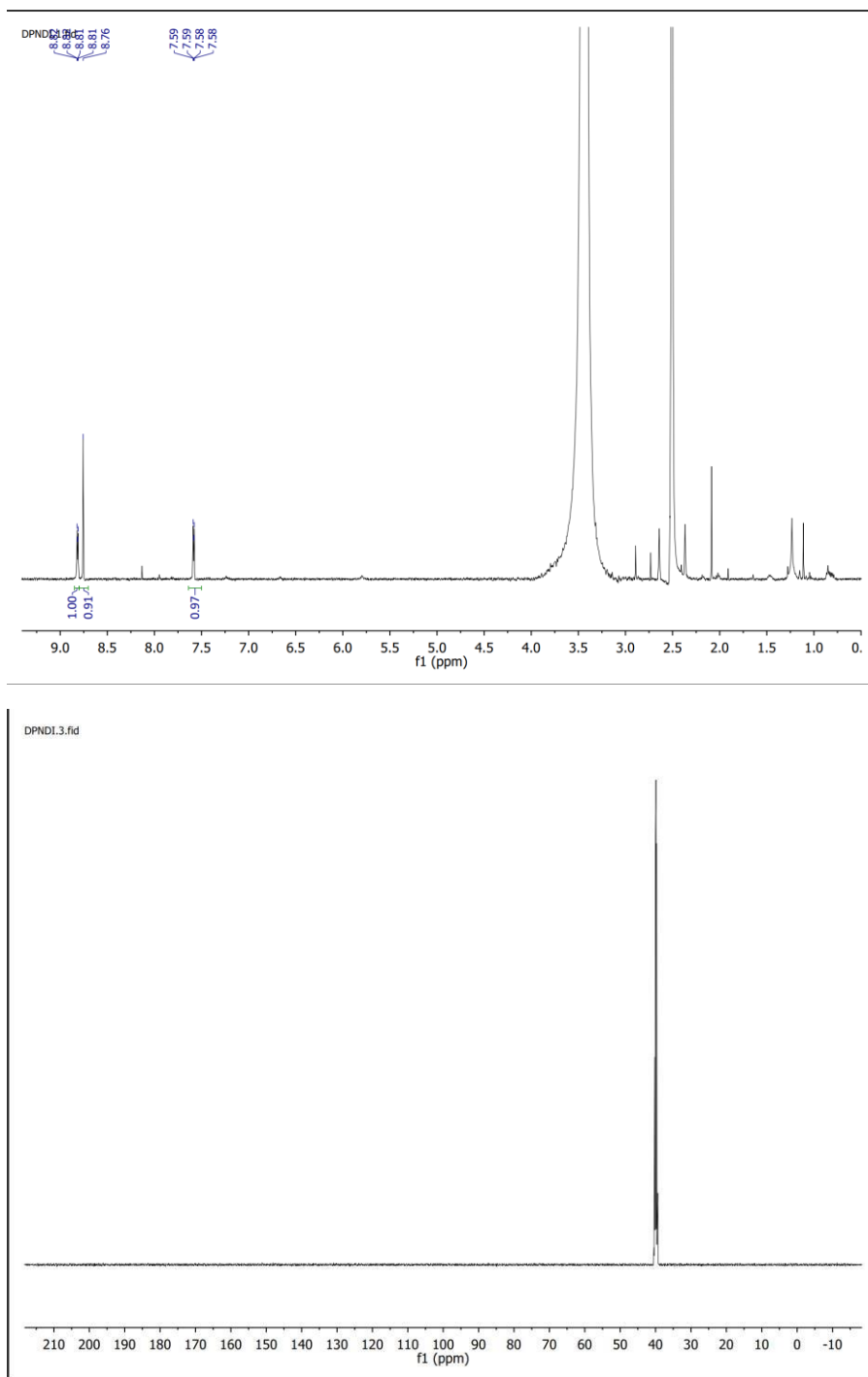


Figure 14: H-NMR (top) and C¹³-NMR (bottom) study of *N,N'*-bis(4-pyridyl)-naphthalene diimide (1) confirmed the product.

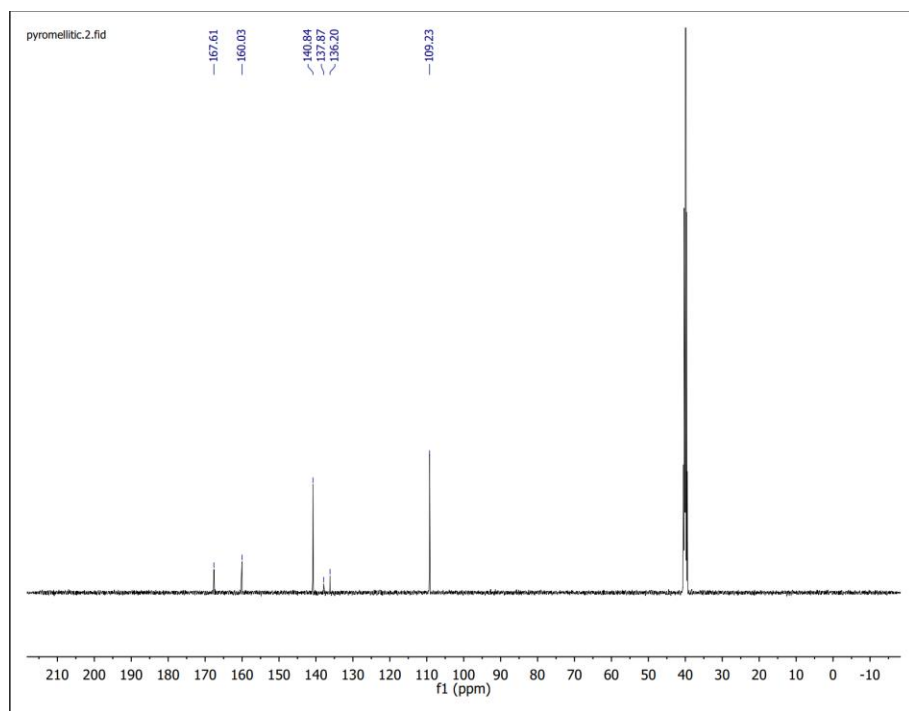
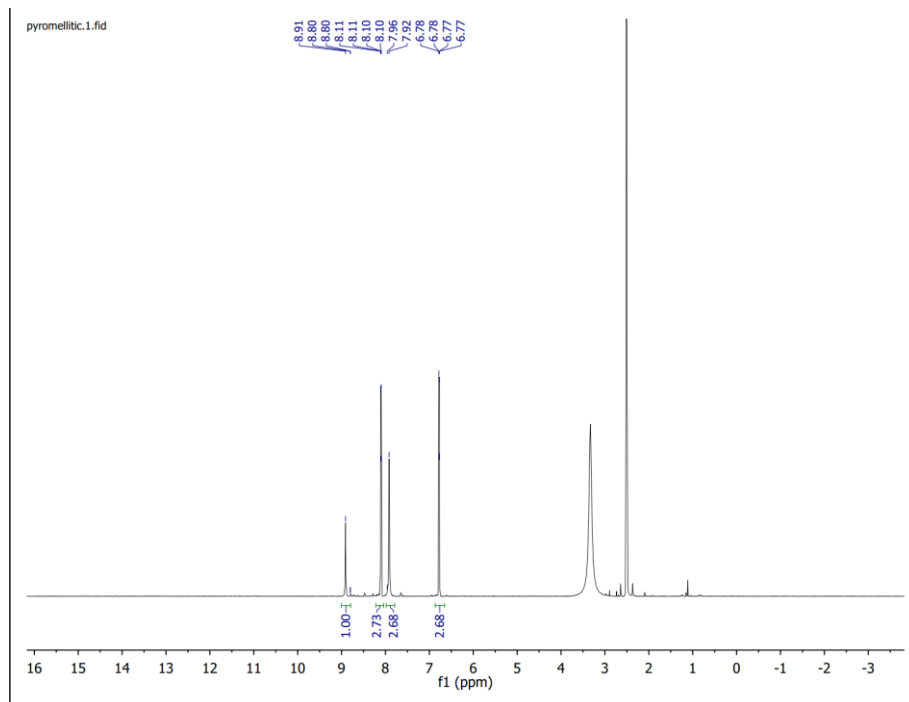


Figure 15: ^1H -NMR (top) spectrum of N,N' -bis(4-pyridyl)-pyromellitic diimide (**3**) (refluxed in DMF) with the excess peaks ascribed to minor impurities. The ^{13}C -NMR spectrum (bottom) also confirmed the formation of the target product.

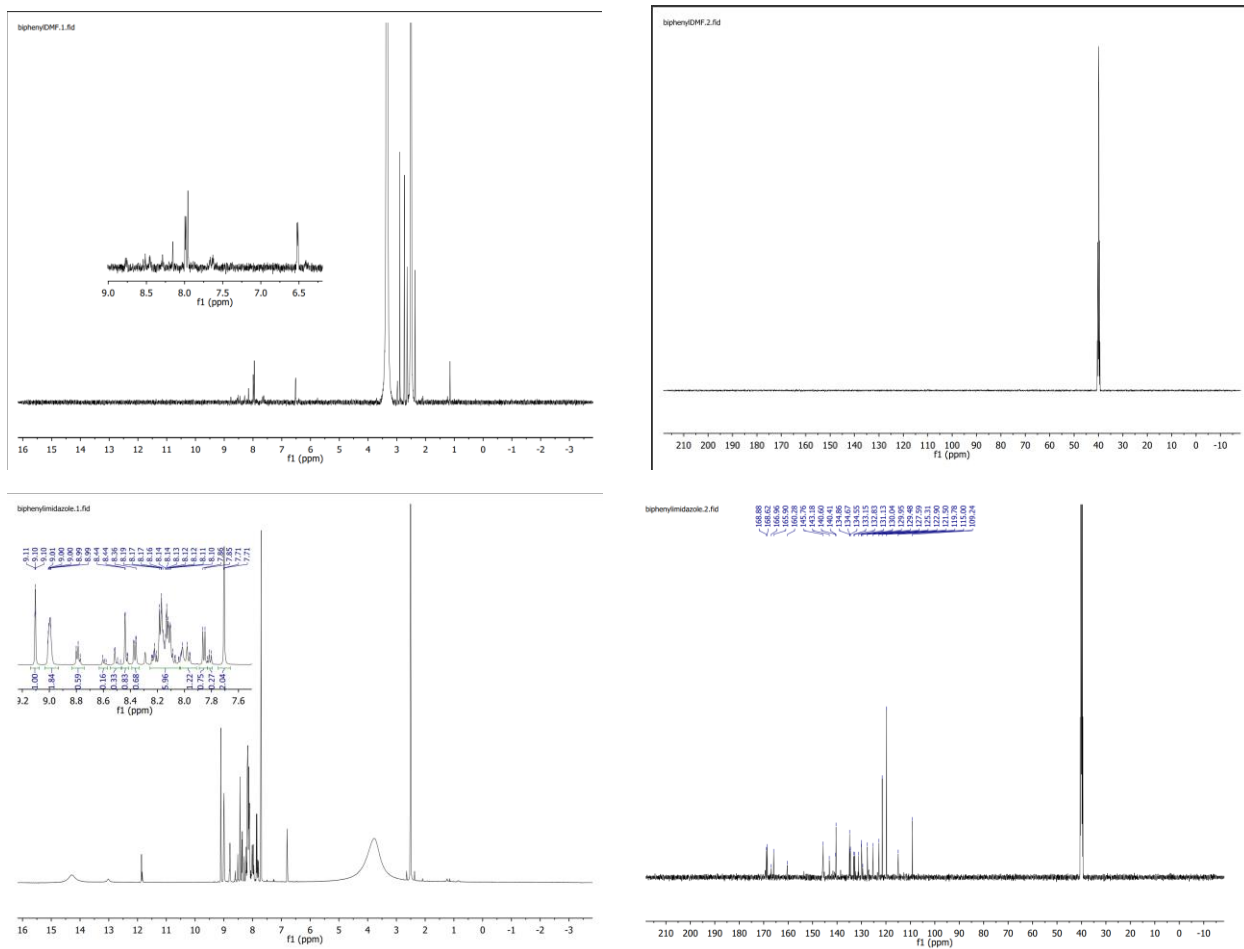
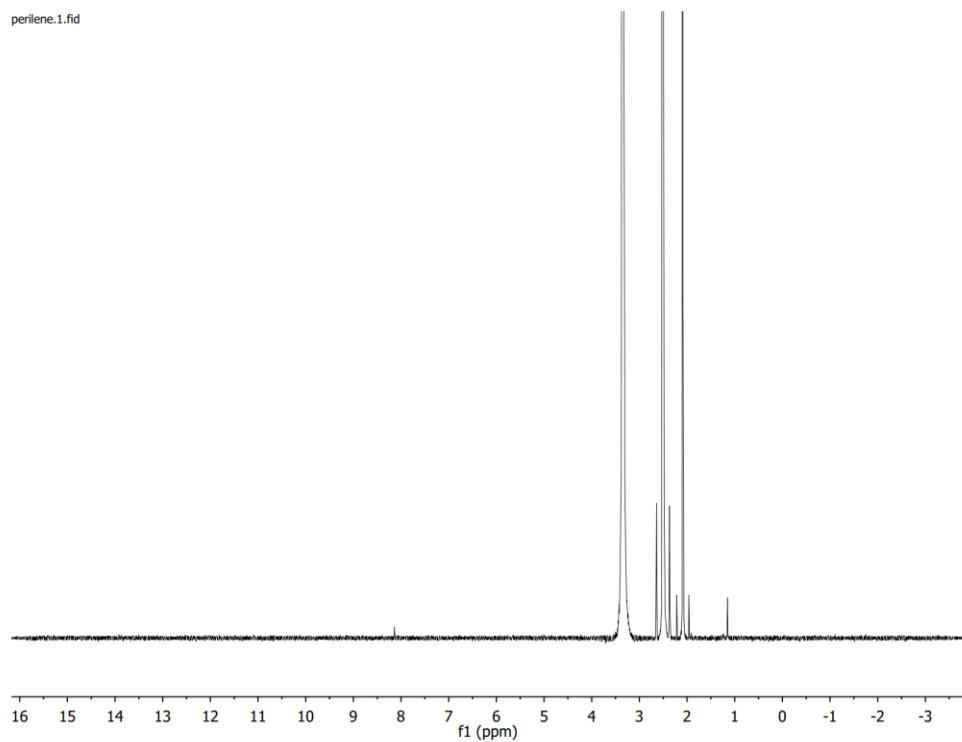


Figure 16: H-NMR and C13-NMR spectra of the *N,N'*-bis(4-pyridyl)-biphenyl diimide (2) (synthesized in DMF) (top). H-NMR and C13-NMR spectra of the impured product (synthesized in imidazole) (bottom).

perilene.1.fid



perilene.2.fid

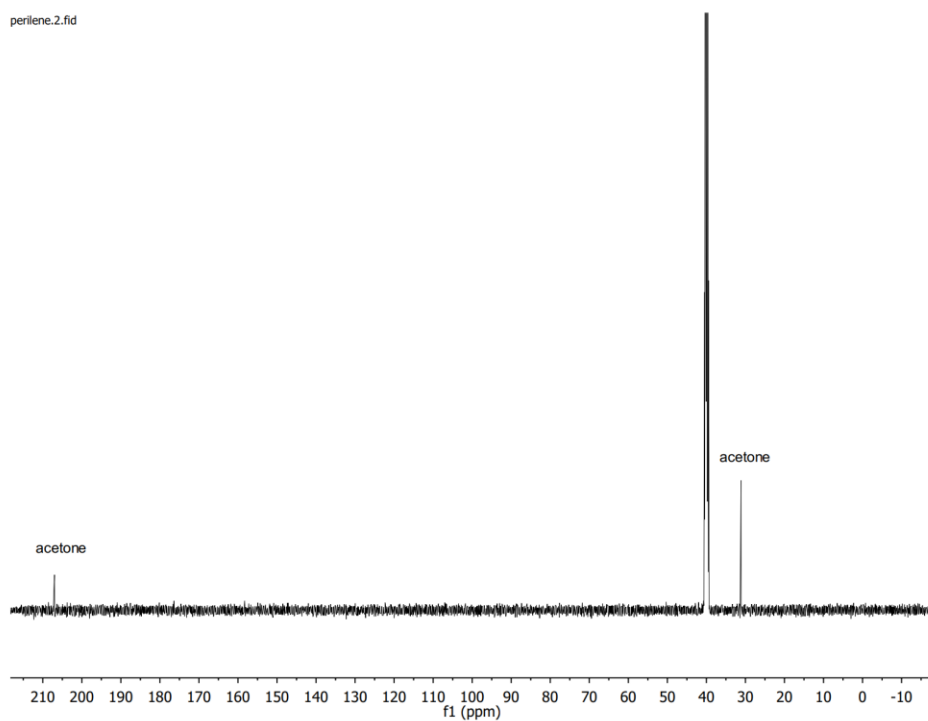


Figure 17: The H-NMR (top) and C¹³-NMR (bottom) spectra for the synthesis of N,N'-bis(4-pyridyl)perylene diimide (4) compound did not confirm the desired product. The peaks correspond to the acetone peaks.

3.4 UV-Vis Spectra

UV-Vis absorption study shown in Figure 18 supports our claim for the production of *N,N'*-bis(4-pyridyl)-naphthalene diimide (**1**) as the two peaks at 380 and 359 nm match the expected absorbance reported in the literature.⁹ These peaks are attributed to the aromatic backbone of the diimide, the naphthalene rings, and the pyridine side chain.

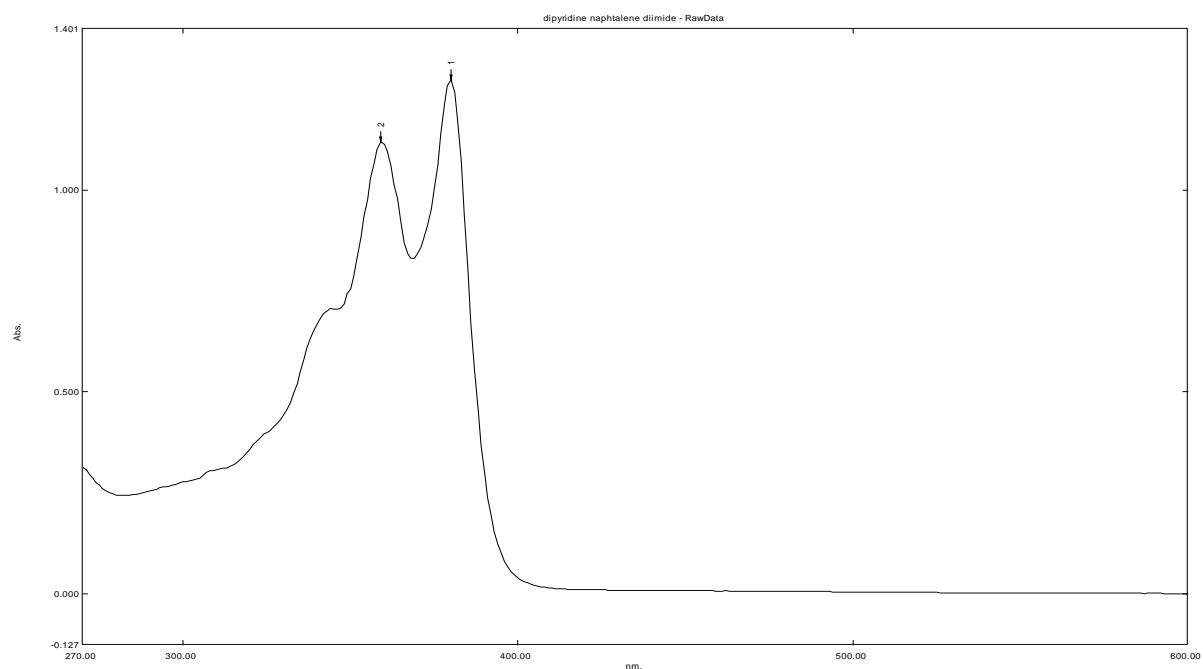


Figure 18: UV-Vis absorbance of *N,N'*-bis(4-pyridyl)-naphthalene diimide (**1**) shows peaks due to the aromatic pyridine side chain as well as the aromaticity of the naphthalene backbone.

The UV-Vis spectroscopy on *N,N'*-bis(4-pyridyl)-pyromellitic diimide (**3**) (see Figure 19) demonstrates that the products synthesized by in both DMF and imidazole yielded similar result as all spectra had a prominent peak at 267 nm. This peak is attributed to the benzene aromatic group in the pyromellitic back bone as well as the pyridine side chains.

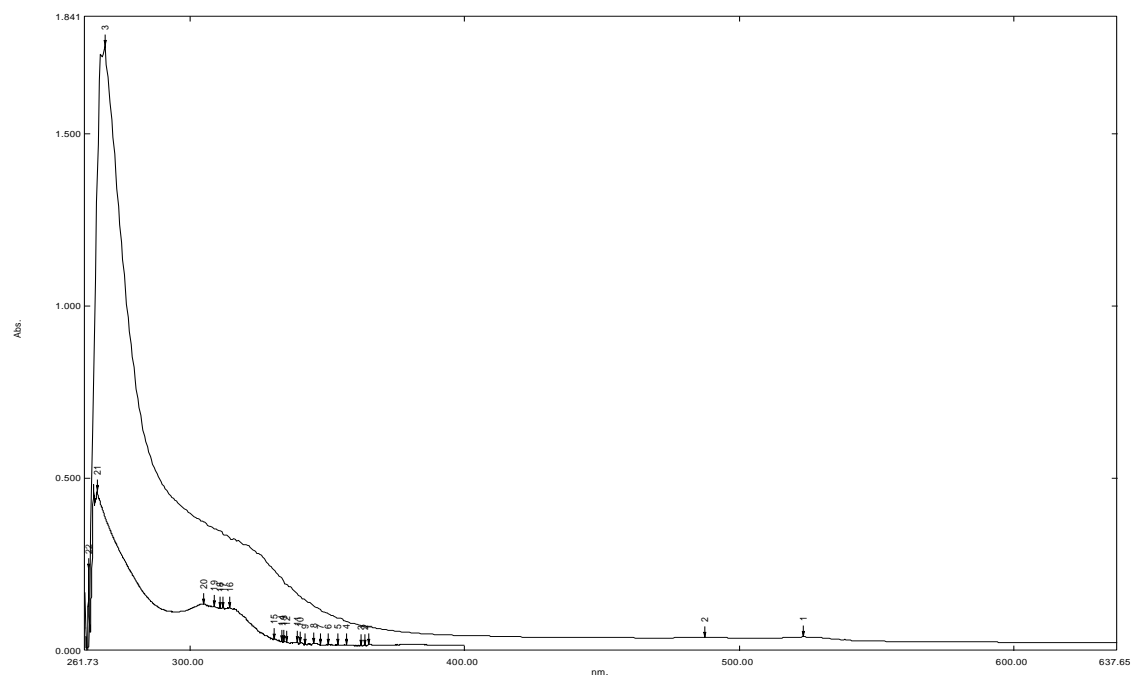


Figure 19: UV-Vis absorbance of *N,N'*-bis(4-pyridyl)-pyromellitic diimide (3) products (synthesized in DMF or Imidazole). These are expected to give the single large peak shown around 269 nm.

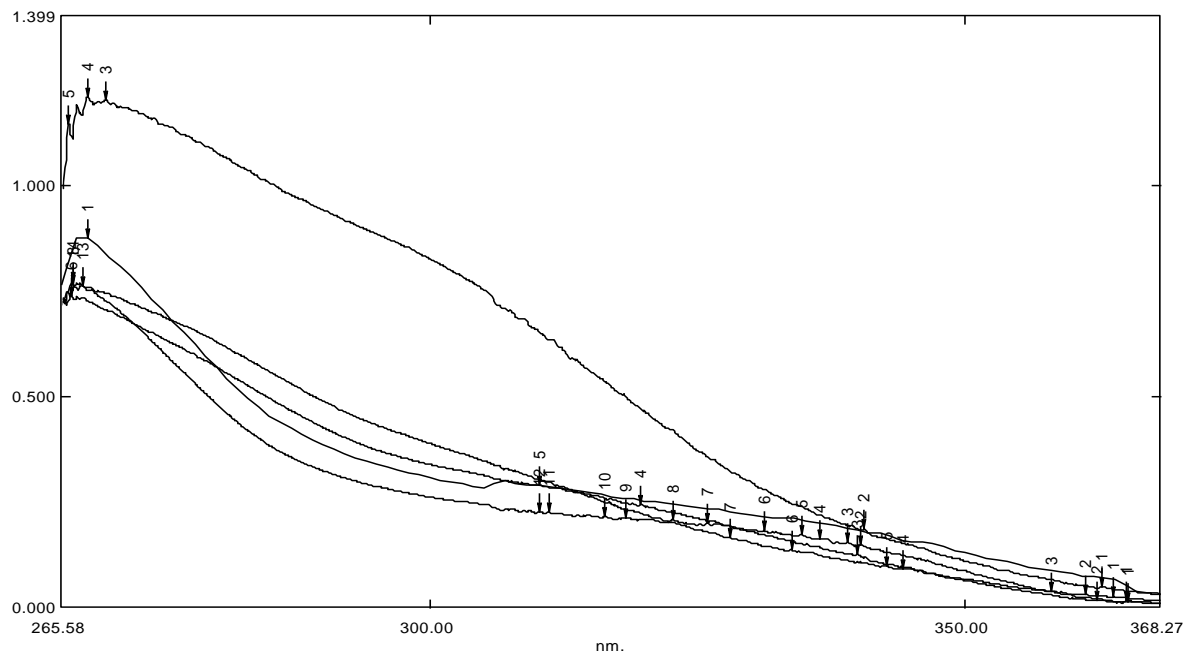


Figure 20: UV-Vis absorbance of *N,N'*-bis(4-pyridyl)-biphenyl diimide (2) compound synthesized in imidazole or DMF – patterns from different batches are similar.

UV-Vis absorbance of N,N'-bis(4-pyridyl)-biphenyl diimide (**2**) (see Figure 20) demonstrates that all different batches from DMF/imidazole-synthesized products have similar compound. The peak around 268 is attributed to the aromatic nature of the symmetrical pyridine and biphenyl rings. This factors into the prominent peak observed like N,N'-bis(4-pyridyl)-pyromellitic diimide (**3**).

UV-Vis spectra of N,N'-bis(4-pyridyl)-perylene diimide (**4**) shown in Figure 21 is indicative of a promising structure. The two peaks in the visible region, 522 nm and 490 nm, are expected to give the dark red color of the product. Further down toward 263 nm this peak is attributed toward the perylene aromatic group as well as the pyridine groups.

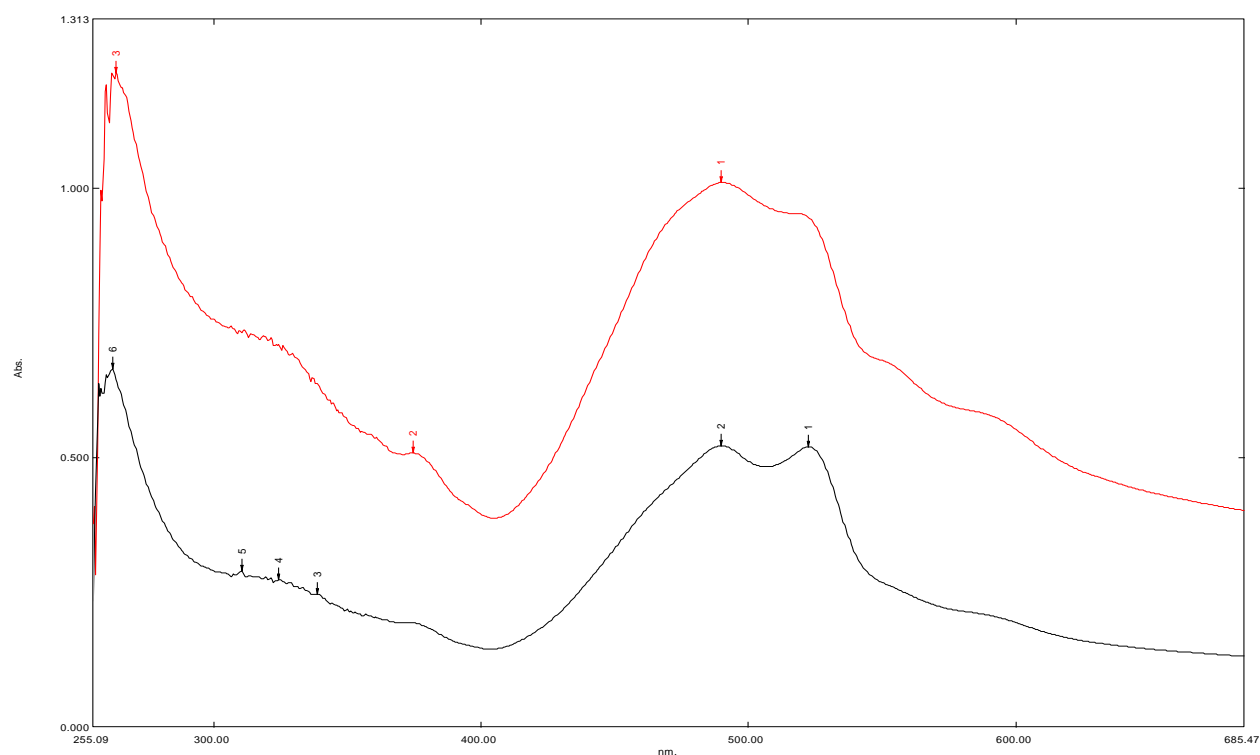


Figure 21: UV-Vis spectra of N,N'-bis(4-pyridyl)-perylene diimide (**4**) compounds indicate that the batches synthesized with imidazole are the same compound with the expected broad peaks at ~500 nm.

Now that we have established a reasonable synthesis method for our ligands, we hope to produce coordination polymers that take advantage of the various structural properties of our compounds. Ultimately, we will use our ligands in complexes with metal ions for proton conductivity studies. Transition metals such as silver¹¹ and iron¹² have proven to yield results in the field of proton conductivity. As a result, metals such as cadmium, manganese, and zirconium are being used in our polymer synthesis to ascertain viable crystallinity and properties. Ions capable of forming multiple oxidation states are believed to be promising precursor for these types of materials. By allowing metal ions to interchange electrons charge, interactions between molecules permits the flow of protons through the molecule. The aromatic groups allow for this as well as the conjugation of π bonds. This is also demonstrated in compounds such as squaric acid derivatives.¹³ For this reason, we have focused on aromatic compounds as the backbone and side chains for our ligands. Specifically, it has been seen that pyridine is conducive to effective proton conductivity when complexed with Cu(II)¹⁴. Based on this the structure of our ligands is thought to be favorable for our purposes. The structural rigidity of aromatic rings also allows for our compounds to be usable without the need of water. Anhydrous environments have been a struggle to overcome as mentioned before. By varying our starting material from the single ring of pyromellitic dianhydride up to the bulky structure of perylene dianhydride we hope to discover the best structure for proton conduction. An appropriate ratio between flexibility and support would allow us to control the interpenetration seen in polymer structure and fine tune for our desired use.

Currently we are still in the synthesis phase of our study and have yet to establish a variety of polymers for study. We are hopeful that the most recently synthesized products will be conducive for x-ray crystallographic study. Previous attempts have shown that using a templating molecule along with our synthesis results in better crystallinity. The use of DMF is expected to not only serve as a solvent for the synthesis of crystal structures but to also fill the pores. Thereafter, the DMF will be replaced with protogenic guest molecules such as imidazole, this would help maintain the environment anhydrous.

3.5 $\{[(\text{CH}_3)_2\text{NH}_2]_2[\text{Zn}\{\text{O}_3\text{PC}_6\text{H}_2(\text{OH})_2\text{PO}_3\}]\}_n$ (5) Structure

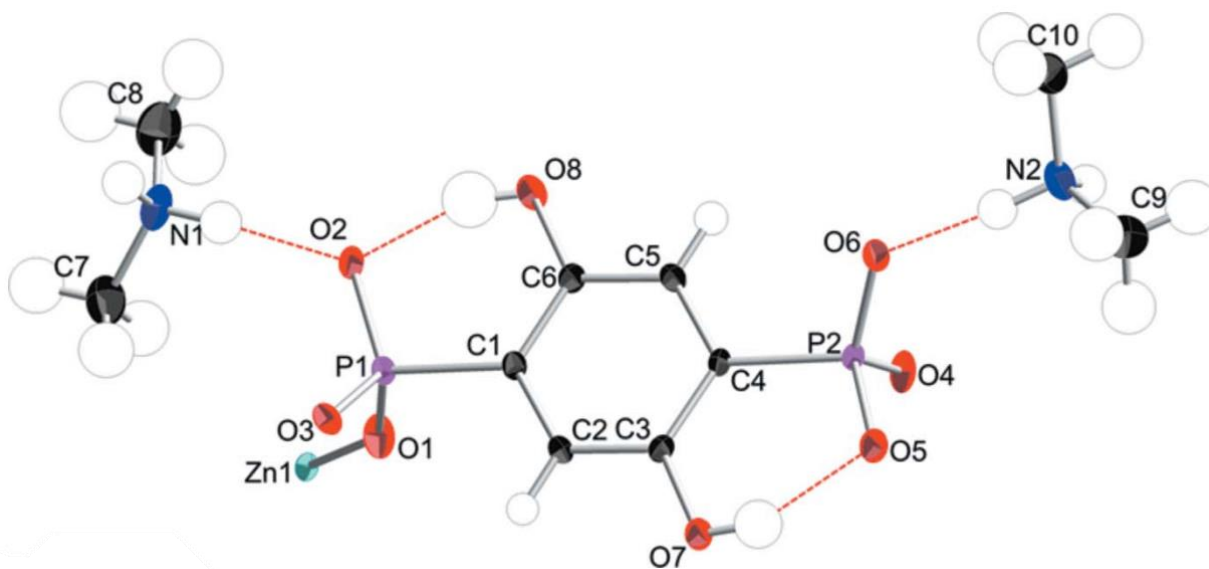


Figure 22: The asymmetric unit of (5) in position $1-x, 1-y, 1-z$ showing 50% displacement ellipsoids.

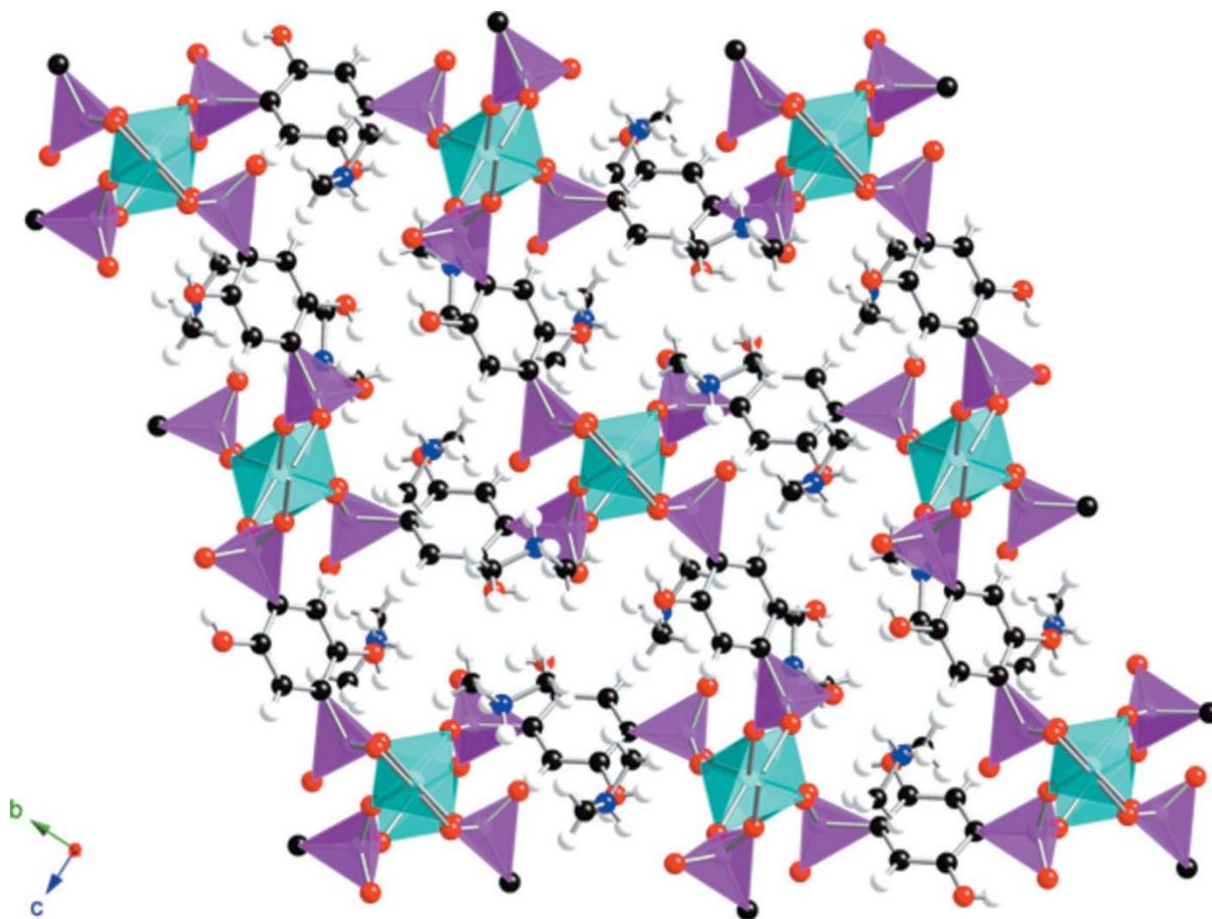


Figure 23: View down [100] of the three-dimensional framework structure of (**5**) with the ZnO_4 and PO_3C moieties shown as polyhedra. Color key: ZnO_4 groups = cyan, PO_3C groups = magenta, oxygen = red, carbon = black, hydrogen = white. The $(\text{CH}_3)_2\text{NH}_2^+$ cations are omitted for clarity.

We have been able to synthesize a phosphonic acid-based polymer. The structure of $\{[(\text{CH}_3)_2\text{NH}_2]_2[\text{Zn}\{\text{O}_3\text{PC}_6\text{H}_2(\text{OH})_2\text{PO}_3\}]\}_n$ (**5**) crystallizes in the monoclinic space group $P2_1/n$ (Table 2). The asymmetric unit contains one Zn^{2+} cation, a $\text{C}_6\text{H}_4\text{P}_2\text{O}_8^{4-}$ hydroxyphosphonate tetra-anion and two $(\text{CH}_3)_2\text{NH}_2^+$ cations (Figure 22). Four rigid phenyl spacers coordinate the three-dimensional framework via the O atoms and tetrahedral ZnO_4 units (Figure 23). The PO_3^{2-} moieties are coordinated by two of their oxygen atoms to Zn^{2+} while the others (O2 and O6) are

not. The distances between Zn-O bonds ranges from 1.9055 to 1.9671 Å and the hydroxyphosphonate ligand in (**5**) contains P-O bonds within a range of 1.5129 - 1.5337 Å. The latter bond lengths are within the expected range for deprotonated P—O bonds.¹⁶ The structure of (**5**) is like {[Zn(DHBP)](DMF)₂}¹⁶ as both frameworks are comprised of one dimensional channels occupied by guest molecules with the difference that {[Zn(DHBP)](DMF)₂}¹⁶ has neutral DMF and the phosphonate groups are singly, rather than doubly deprotonated. The channels reported for (**5**) compound are smaller than those for {[Zn(DHBP)](DMF)₂} measuring approximately 12.9 X 7.1 Å between phenyl groups and 9.9 Å between Zn centers. The (CH₃)₂NH₂⁺ cations in (**5**) have been formed by the *in situ* decarbonylation of the DMF solvent. It is known that N,N-dimethylformamide can undergo loss of CO to form dimethylamine in the presence of a metal catalyst or through slow decomposition at elevated temperature around 427 K.¹⁷⁻²⁰ In the previous reports, the nitrate salts of Mg²⁺/Pb²⁺/Ho³⁺ and chloride salts of Nd³⁺/Zr⁴⁺ were suggested to act as a metal catalyst in the decarbonylation of the DMF solvent. The C6—O8H and C3—O7H groups appended on the phenyl ring of the ligand form intramolecular O—H···O hydrogen bonds with the adjacent RPO₃²⁻ moieties (Figure 22). Within the channels, the (CH₃)₂NH₂⁺ cations are linked by N—H···O hydrogen bonds to the RPO₃²⁻ groups of the framework (Table 1). Some short C—H···O contacts (Table 1) may help to consolidate the structure.

Table 1
Hydrogen-bond geometry (Å, °).

$D-H\cdots A$	$D-H$	$H\cdots A$	$D\cdots A$	$D-H\cdots A$
O7—H7A···O5	0.79 (2)	1.91 (2)	2.6510 (17)	156 (3)
O8—H8A···O2	0.87 (3)	1.73 (3)	2.5846 (18)	168 (3)
N1—H1A···O2	0.89 (2)	1.88 (2)	2.7168 (19)	155.2 (18)
N1—H1B···O6 ⁱ	0.89 (2)	2.02 (2)	2.8125 (19)	148.3 (18)
N2—H2B···O3 ⁱⁱ	0.83 (3)	2.07 (3)	2.8558 (19)	158 (2)
N2—H2C···O6	1.03 (2)	1.63 (2)	2.6518 (18)	173 (2)
C7—H7C···O4 ⁱⁱⁱ	0.91 (2)	2.54 (2)	3.443 (3)	174 (2)
C9—H9B···O8 ^{iv}	1.03 (3)	2.57 (2)	3.445 (3)	142.6 (19)
C10—H10A···O8 ^{iv}	0.92 (3)	2.42 (3)	3.236 (3)	148 (3)

Symmetry codes: (i) $-x + 1, -y + 1, -z + 1$; (ii) $x + \frac{1}{2}, -y + \frac{3}{2}, z + \frac{1}{2}$; (iii) $-x + \frac{3}{2}, y - \frac{1}{2}, -z + \frac{1}{2}$; (iv) $-x + \frac{3}{2}, y + \frac{1}{2}, -z + \frac{3}{2}$.

TABLE 2

Crystallographic Data For $\{[(\text{CH}_3)_2\text{NH}_2]_2[\text{Zn}\{\text{O}_3\text{PC}_6\text{H}_2(\text{OH})_2\text{PO}_3\}]\}_n$ (**5**)

Formula Mass	423.59
Color and Habit	colorless
Space Group	<i>Monoclinic P2₁/n</i>
<i>a</i> (Å)	8.8455(5)
<i>b</i> (Å)	16.4492(9)
<i>c</i> (Å)	11.2721(6)
α (°)	90
β (°)	97.338(1)
γ (°)	90
<i>V</i> (Å ³)	1626.67(15)
<i>Z</i>	4
<i>T</i> (K)	220
λ (Å)	0.71073
ρ_{calcd} (g cm ⁻³)	1.730
μ (Mo K α) (mm ⁻¹)	1.75
$R(F)$ for $F_o^2 > 2\sigma(F_o^2)^a$	0.022
$R_w(F_o^2)^b$	0.0273

$$^a R(F) = \frac{\sum \left| |F_o| - |F_c| \right|}{\sum |F_o|}, \quad ^b R_w(F_o^2) = \left[\frac{\sum \left[w(F_o^2 - F_c^2)^2 \right]}{\sum wF_o^4} \right]^{1/2}$$

CHAPTER 4: CONCLUSIONS

Based on the data collected, the belief that I could successfully synthesize the target ligands for the future production of MOFs is supported for all the compounds synthesized except N,N'-bis(4-pyridyl)-perylene diimide (**4**). Perylene compounds resulted in minimal yield when both imidazole and DMF were used as solvents. In fact, the DMF synthesis failed entirely, leading us to conclude that a different synthetic method should be used in order to produce the desired compounds. Future study is needed to determine what solvent would be sufficient for the synthesis of compound **4**. Imidazole was successful in synthesizing most of the target compounds. Aside from the products obtained for N,N'-bis(4-pyridyl)-naphthalene diimide (**1**), the yields were generally poor. The yields were high whenever DMF was used in all the synthesis performed. It is important to conclude that an optimized imidazole synthesis could be used on account of the shorter refluxing time while the synthesis in DMF provide the pathway to better yields thus offsetting the time difference in the two synthetic methods.

On account of the synthesis of $\{[(\text{CH}_3)_2\text{NH}_2]_2[\text{Zn}\{\text{O}_3\text{PC}_6\text{H}_2(\text{OH})_2\text{PO}_3\}]\}_n$ (**5**), more research should be conducted into the mechanism of decarbonylation of DMF *in situ*. Taking the current known mechanism for this process it would be beneficial to study the effects of DMF as a solvent in future coordination polymer synthesis for proton conductivity research.

CHAPTER 5:

REFERENCES

- (1) Castaldelli, E.; Imalka Jayawardena, K. D. G.; Cox, D. C.; Clarkson, G. J.; Walton, R. I.; Le-Quang, L.; Chauvin, J.; Silva, S. R. P.; Demets, G. J.-F. Electrical Semiconduction Modulated by Light in a Cobalt and Naphthalene Diimide Metal-Organic Framework. *Nat. Commun.* **2017**, *8*. <https://doi.org/10.1038/s41467-017-02215-7>.
- (2) Rao, K. V.; Haldar, R.; Kulkarni, C.; Maji, T. K.; George, S. J. Perylene Based Porous Polyimides: Tunable, High Surface Area with Tetrahedral and Pyramidal Monomers. *Chem. Mater.* **2012**, *24* (6), 969–971. <https://doi.org/10.1021/cm203599q>.
- (3) Farha, O. K.; Malliakas, C. D.; Kanatzidis, M. G.; Hupp, J. T. Control over Catenation in Metal–Organic Frameworks via Rational Design of the Organic Building Block. *J. Am. Chem. Soc.* **2010**, *132* (3), 950–952. <https://doi.org/10.1021/ja909519e>.
- (4) Haque, E.; Jun, J. W.; Jhung, S. H. Adsorptive Removal of Methyl Orange and Methylene Blue from Aqueous Solution with a Metal-Organic Framework Material, Iron Terephthalate (MOF-235). *J. Hazard. Mater.* **2011**, *185* (1), 507–511. <https://doi.org/10.1016/j.jhazmat.2010.09.035>.
- (5) Sang, L.; Cheng, Y.; Yang, R.; Li, J.; Kong, Q.; Zhang, J. Polyphosphazene-Wrapped Fe–MOF for Improving Flame Retardancy and Smoke Suppression of Epoxy Resins. *J. Therm. Anal. Calorim. Int. Forum Therm. Stud.* **2021**, *144* (1), 51. <https://doi.org/10.1007/s10973-020-09481-6>.
- (6) Dinolfo, P. H.; Williams, M. E.; Stern, C. L.; Hupp, J. T. Rhenium-Based Molecular Rectangles as Frameworks for Ligand-Centered Mixed Valency and Optical Electron Transfer. *J. Am. Chem. Soc.* **2004**, *126* (40), 12989–13001. <https://doi.org/10.1021/ja0473182>.
- (7) Pagano, P.; Pelagatti, P.; Bacchi, A.; Chierotti, M. R.; Bourne, S. A.; Mehlana, G. Sorption Properties toward Environmentally Important VOCs of Half-Sandwich Ru(II) Complexes Containing Perylene Bisimide Ligands. *Inorg. Nano-Met. Chem.* **2017**, *47* (3), 427–432. <https://doi.org/10.1080/15533174.2016.1186068>.
- (8) Jensen, S.; Tan, K.; Lustig, W. P.; Kilin, D. S.; Li, J.; Chabal, Y. J.; Thonhauser, T. Structure-Driven Photoluminescence Enhancement in a Zn-Based Metal–Organic Framework. *Chem. Mater.* **2019**, *31* (19), 7933–7940. <https://doi.org/10.1021/acs.chemmater.9b02056>.
- (9) Guha, S.; Goodson, F. S.; Corson, L. J.; Saha, S. Boundaries of Anion/Naphthalenediimide Interactions: From Anion– π Interactions to Anion-Induced Charge-Transfer and Electron-Transfer Phenomena. *J. Am. Chem. Soc.* **2012**, *134* (33), 13679–13691. <https://doi.org/10.1021/ja303173n>.

- (10) Trivedi, D. R.; Fujiki, Y.; Fujita, N.; Shinkai, S.; Sada, K. Crystal Engineering Approach To Design Colorimetric Indicator Array To Discriminate Positional Isomers of Aromatic Organic Molecules. *Chem. - Asian J.* **2009**, *4* (2), 254–261. <https://doi.org/10.1002/asia.200800341>.
- (11) Yang, L.; Li, X.; Qin, C.; Wang, X.-L.; Shao, K.-Z.; Su, Z.-M. A Highly Electrical Conducting, 3D Supermolecular Ag(I) Coordination Polymer Material with Luminescent Properties. *Inorg. Chem. Commun.* **2016**, *70*, 31–34. <https://doi.org/10.1016/j.inoche.2016.04.010>.
- (12) Meng, Y.; Dong, Y.-J.; Yan, Z.; Chen, Y.-C.; Song, X.-W.; Li, Q.-W.; Zhang, C.-L.; Ni, Z.-P.; Tong, M.-L. A New Porous Three-Dimensional Iron(II) Coordination Polymer with Solvent-Induced Reversible Spin-Crossover Behavior. *Cryst. Growth Des.* **2018**, *18* (9), 5214–5219. <https://doi.org/10.1021/acs.cgd.8b00657>.
- (13) Basak, D.; Versek, C.; Toscano, D. T.; Christensen, S.; Tuominen, M. T.; Venkataraman, D. Anhydrous Proton Conductivities of Squaric Acid Derivatives. *Chem. Commun.* **2012**, *48* (47), 5922. <https://doi.org/10.1039/c2cc31283b>.
- (14) Wei, M.; Chen, L.; Duan, X. A Porous Cu(II)-MOF Containing [PW 12 O 40] and a Large Protonated Water Cluster: Synthesis, Structure, and Proton Conductivity. *J. Coord. Chem.* **2014**, *67* (17), 2809–2819. <https://doi.org/10.1080/00958972.2014.957689>.
- (15) Soriano, J. S.; Galeas, B. E.; Garrett, P.; Flores, R. A.; Pinedo, J. L.; Kohlgruber, T. A.; Felton, D.; Adelani, P. O. In Situ Decarbonylation of N,N-Dimethylformamide to Form Dimethylammonium Cations in the Hybrid Framework Compound $\{[(\text{CH}_3)_2\text{NH}_2]_2[\text{Zn}\{\text{O}_3\text{PC}_6\text{H}_2(\text{OH})_2\text{PO}_3\}]\}_n$. *Acta Crystallogr. Sect. E* **2019**, *75* (10), 1540–1543. <https://doi.org/10.1107/S2056989019012969>
- (16) Liang, J.; Shimizu, G. K. H. Crystalline Zinc Diphosphonate Metal–Organic Framework with Three-Dimensional Microporosity. *Inorg. Chem.* **2007**, *46* (25), 10449–10451. <https://doi.org/10.1021/ic701628f>.
- (17) Hulushe, S. T.; Hosten, E. C.; Watkins, G. M. Dimethylammonium 2,4,5-Tricarboxybenzoate: An Example of the Decarbonylation of N, N-Dimethylformamide in the Presence of a Metal and a Benzenepolycarboxylic Acid. Is Zirconium(IV) the *Tsotsi*? *Acta Crystallogr. Sect. E Crystallogr. Commun.* **2016**, *72* (11), 1521–1525. <https://doi.org/10.1107/S2056989016014948>.
- (18) Siddiqui, T.; Koteswara Rao, V.; Zeller, M.; Lovelace-Cameron, S. R. Dimethylammonium 3-Carboxybenzoate. *Acta Crystallogr. Sect. E Struct. Rep. Online* **2012**, *68* (6), o1778–o1778. <https://doi.org/10.1107/S160053681202096X>.
- (19) Chen, D.-C.; Li, X.-H.; Ding, J.-C. Bis(Dimethylammonium) 2,5-Dicarboxybenzene-1,4-Dicarboxylate Bis(1,10-Phenanthroline). *Acta Crystallogr. Sect. E Struct. Rep. Online* **2007**, *63* (3), o1133–o1135. <https://doi.org/10.1107/S1600536807004783>.

(20) Karpova, E. V.; Zakharov, M. A.; Gutnikov, S. I.; Alekseyev, R. S.
Bis(Dimethylammonium) Terephthalate. *Acta Crystallogr. Sect. E Struct. Rep. Online* **2004**, *60*
(12), o2491–o2492. <https://doi.org/10.1107/S1600536804028685>.